Deconstructing SARS-CoV-2 neutralization: A modular molecular framework for computational design and comparison of antibodies and nanobodies targeting the spike RBD

Vincenzo Tragni[1] | Ivan Mercurio[2] | Diletta Pia Paoletti[2] | Angelo Onofrio[1] | Luna Laera[2] | Lucas Cafferati Beltrame[2] | Maria Noemi Sgobba[2] | Lorenzo Guerra[2] | Mariateresa Volpicella[2] | Anna De Grassi[2] | Gabriella Elia[3] | Ciro Leonardo Pierri[1]

Abstract

Since 2020 the COVID-19 pandemic has led scientists to search for strategies to predict the transmissibility and virulence of new severe acute respiratory syndromecoronavirus 2 variants based on the estimation of the affinity of the spike receptor binding domain (RBD) for the human angiotensin-converting enzyme 2 (ACE2) receptor and/or neutralizing antibodies. In this context, our lab developed a computational pipeline to quickly quantify the free energy of interaction at the spike RBD/ACE2 protein–protein interface, reflecting the incidence trend observed in thetransmissibility/virulence of the investigated variants. In this new study, we used our pipeline to estimate the free energy of interaction between the RBD from 10 variants, and 14 antibodies (ab), or 5 nanobodies (nb), highlighting the RBD regionspreferentially targeted by the investigated ab/nb. Our structural comparative analysis and interaction energy calculations allowed us to propose the mostpromising RBD regions to be targeted by future ab/nb to be designed by site- directed mutagenesis of existing high-affinity ab/nb, to increase their affinity for the target RBD region, for preventing spike-RBD/ACE2 interactions and virus entry in host cells. Furthermore, we evaluated the ability of the investigated ab/nb to simultaneously interact with the three RBD located on the surface of the trimericspike protein, which can alternatively be in up- or down- (all-3-up-, all-3-down-, 1-up-/2-down-, 2-up-/1-down-) conformations.

KEYWORDS

antibody receptor interactions, antiviral research, binding affinity, interaction energyprediction, nanobodies, neutralizing antibodies, SARS-CoV-2, SARS-CoV-2 variants

[1]Department of Pharmacy—Pharmaceutical Sciences, University of Bari, Bari, Italy

[2]Department of Biosciences, Biotechnologies, Environment, University of Bari, Bari, Italy

[3]Department of Veterinary Medicine, University of Bari, Valenzano, Italy

Correspondence

Ciro Leonardo Pierri, Department of Pharmacy —Pharmaceutica Sciences, University of Bari, via Orabona, 4, 70125 Bari, Italy.
Email: ciro.pierri@uniba.it

Funding information

EU funding within the MUR PNRR National Center for Gene Therapy and Drugs based on RNA Technology (Project no. CN_00000041); EU funding within the MUR PNRR Extended Partnership initiative on Emerging Infectious Diseases (Project no. PE00000007, INF-ACT)

Abbreviations: Ab, antibody; ACE2, human dipeptidyl carboxydipeptidase angiotensin converting enzyme II; Covid-19, coronavirus disease 2019; H-bonds, hydrogen-bonds; nb, nanobody; PDB, Protein Data Bank; RBD, receptor binding domain; SARS-CoV-2, severe acute respiratory syndrome; VoC, variants of concern.

Vincenzo Tragni and Ivan Mercurio have equal contribution.

1 | INTRODUCTION

Severe acute respiratory syndrome coronavirus 2 (SARS-CoV-2) infection main actor is undoubtedly represented by the spike protein widely distributed on the virus surface. This protein is used by the virus to scan the host-cell surface searching for the human host-cell main interactor, represented by angiotensin-converting enzyme 2 (ACE2) receptor.[1–3] As stable protein–protein interactions between the SARS-CoV-2 spike protein and ACE2 are established, membrane fusion events are triggered, allowing virus entry into the human host-cells.[1–5] The spike protein is a homotrimeric protein complex, with each monomer consisting of an N-terminal (S1) subunit that contains the roughly 200-residue receptor binding domain (RBD), and aC-terminal subunit (S2) containing the fusion protein.[2,3,5] The SARS-CoV-2 spike protein is responsible for virus-cell entry through interactions with the human dipeptidyl carboxydipeptidase ACE2 receptor, which represents the main source of interactions between SARS-CoV-2 and proteins on the surface of human cells.[1–4,6,7] Each monomer of the trimeric SARS-CoV-2 spike protein has a boat-shaped RBD[3] involved in interactions with the human ACE2 receptor, to facilitate virus entry into the human host cell. While the virus scans the surface of the host-cells by using the spike protein searching for interactions with ACE2, the spike RBD can be more or less exposed, allowing the spike protein to adopt a more open conformation with all the three RBD in up-conformation or a closed conformation with the three RBD in down-conformation. These conformational changes seem to depend on the pH of the specific tissue invaded by the virus.[8] Two other conformations have been observed showing the spike protein with 2 RBD in up- and 1 RBD in down- or 2 RBD in down- and 1 RBD in up- conformation.[1–7,9] In the absence of ACE2, it was observed that the RBD orientation is sensitive to pH variations. Indeed, spike proteins showing a single RBD in up-conformation are observed at pH 5.5, whereas an all-down-conformation can be observed at lower pH.[1,2,4,9] Importantly, a pH-dependent refolding region (residues 824–858) at the spike-intermonomer interface displays dramatic structural rearrangements and mediates RBD orientation through coordinated movements of the entire trimer apex.[2,4,9]

In the current scenario of the COVID-19 pandemic, a great help has come from the developed vaccines,[10] based on the spike protein, for stimulating the production of antibodies (ab) to prevent spike/ACE2 protein-protein interactions. It was shown that most of the produced ab target the RBD, which appears to be the most accessible spike region, partly due to the high flexibility of the three RBD boat-shaped lobes.[1] Conversely, the rise of new variants showing missense mutations at the spike RBD has improved the ability of those variants to evade ab produced by vaccines based on the native spike proteinof the Wuhan sequence or infections caused by previous variants.[2,3,11–18] Among the recent variants, the high transmissibility demonstrated by Omicron-derived variants has made it necessary to update the previous messenger RNA (mRNA) based vaccines with omicron variant spike mRNA, leading to the recent Food and Drug Administration approval of bivalent vaccines.[19]

To counteract the virus spread a few antiviral small molecules, i.e., paxlovid (consisting of Nirmatrelvir with ritonavir[20]), molnupiravir,[21] and fluvoxamine,[22] have been investigated in clinical trials and approved as drugs.[23] However, questions have arisen regarding whether the approved small molecules help individuals who are not at high risk of serious disease. Similarly, the efficacy of those small molecules against the newly spreading variants remains questionable.

Thus, there is still an urgent need to develop a potent/versatile dedicated antiviral treatment. In this regard, a combination of monoclonal ab or nanobodies (nb), to be easily modified to increase their activity against specific variants, continues to appear as an attractive/valid approach[24] to address the unmet therapeutical/medical demands[2,3,11–18] associated with the rise of new variants, which periodically lead to increased virus transmissibility, virulence, and patient hospitalization.

The employment of efficient monoclonal ab or nb aims to prevent interactions between SARS-CoV-2 spike RBD and the human receptor ACE2.[2,3,11–18] In this context, a few neutralizing monoclonal ab and nb have already been employed in clinics, and their crystallized structures, in complex with the SARS-CoV-2 spike RBD, have been solved and made available through the protein data bank (PDB). The availability of those structures has two important implications. First, it enables the development of new tools to estimate the binding affinities of the SARS-CoV-2 spike protein for both the human ACE2 receptor[2,3] and the deposited ab or nb.[1,2,4] Second, it allows for the engineering of new ab/nb by in silico/in vitro site-directed mutagenesis of specific ab/nb residues, which may play a crucial role in binding interactions with residues important for SARS-CoV-2 spike RBD/ACE2 or for SARS-CoV-2 spike/ab or spike/nb interactions. The strength of the cited interactions can be quantified by calculating the binding affinity at the protein-protein interface within the deposited structures.[2,3,11–18,24–27] Indeed, starting from the deposited structures, 3D modeling approaches can be used to build reliable 3D models of the spike protein of new variants in complex with ACE2 receptor or ab/nb, as the spike sequences from new variants become available from sequencing platforms. The availability of those 3D models enables the selection of ideal ab/nb mutants with increased affinity for the investigated mutated spike protein.[2,3,11–18,24–27]

In this study, we have improved and integrated our modular molecular framework used for calculating spike RBD/ACE2 free energy of interaction,[2,3] with the aim to build 3D models of the SARS-CoV-2 spike RBD/ab or spike RBD/nb protein complexes, and to calculate spike RBD/ab or spike RBD/nb free energy of interaction.

For our analysis, we selected 19 ab/nb consisting of the ab m396 (2dd8.pdb,[28]) isolated from a convalescent patient infected with SARS-CoV-1, 7 ab derived from convalescent patients or humanized ab such as LY-CoV481, LY-CoV488 (7kmi.pdb and 7kmh.pdb, respectively[26]), CR3022 (6zh9.pdb,[25,29]), CT-P59 (7cm4.pdb,[16]), COVA1.16 and CV503 (7lq7.pdb,[30]) and ADG20 (7u2d.pdb,[31]); 3 ab tested in clinical trials, namely LY-CoV555 (7kmg.pdb,[26]),

REGN10933 and REGN10987 (6xdg.pdb,[15]), and 4 nb, whose structure was recently solved, namely Ty1 (6zxn.pdb,[17]), H11-H4 (6zh9.pdb,[25]), VHH_U and VHH_E (7kn5.pdb,[27]).

Except for m396, crystallized in complex with the RBD of SARS-CoV-1, all the other above-cited ab/nb were crystallized in complex with the RBD of the SARS-CoV-2 spike (Wuhan sequence, according to the YP_009724390.1 sequence) and served as a reference protein sequence. Additionally, the nb C1 and the ab Beta-27, crystallized in complex with the RBD from Omicron BA.5 (7zxu.pdb,[32]), and the ab Beta-55 and EY6A (7qnw.pdb,[33]), crystallized in complex with the RBD from Omicron B.1.1.529, were also considered in our analysis for comparative purposes.

To assess the potential changes in the affinity of the investigated ab/nb for the spike protein of the investigated variants, we considered 10 SARS-CoV-2 variants (including the Wuhan variant). Among these variants, four are classified as variants of concern (VoC), consisting of B.1.351 (known as S. Africa variant, showing the mutations K417N, E484K, N501Y at the RBD), B.1.617 (known as India variant, showing the mutations L452R; E484Q at the RBD), B.1.1.7 (known as UK variant, showing the mutations N501Y, S494P, E484K at the RBD) and P1 (known as Japan/Brazil variant, showing the mutations K417T, E484K, N501Y at the RBD) variants. Three additional variants include B1.141 (showing the mutation N439K at the RBD), B1.620 (showing the mutations S477N, and E484K at the RBD); B.1.427 (known as California variant, showing the mutation L452R at the RBD). Data about the investigated variants can be found on https://www.gisaid.org/ and/or in the following papers.[2,3,11–18,24–27] For each of the cited variants, we constructed the corresponding spike RBD/ab or spike RBD/nb protein complex by in silico mutagenesis and superimposition operations.[2,3,34,35]

Notably, all the cited variant genomes were sequenced in 2021 and were responsible for COVID-19 pandemics situation[14,18,36–40] before the emergence of the Omicron variant. Then, the Omicron-derived variants quickly became the prevalent variants in circulation due to their high transmissibility and relatively lower lethality.[41] In this context, we included in our analysis also the Omicron B.1.1.529 and the Omicron BA.4/5 spike RBD for comparative purposes.

Beyond producing the protein-protein complex structures hosting the spike RBD/ab or the spike RBD/nb protein complex for calculating the interaction energies at the RBD/ab or at the RBD/nb protein-protein interface, for each investigated variant, we also investigated the ability of the investigated ab/nb in targeting simultaneously the three RBD in the four different trimeric spike conformations. These conformations include the spike protein showing all the three RBD in down-conformation, all the three RBD in up-conformation, 1 RBD up- and 2 RBD in down-conformation, 2 RBD up- and 1 RBD in down-conformation. This analysis showed that nb can theoretically better interact simultaneously with different binding regions of different RBD of the same trimeric spike protein, thereby preventing spike RBD/ACE2 interactions in a more efficient way.

2 | MATERIALS AND METHODS

2.1 | Crystallized structures and comparative 3D modeling of SARS-CoV-2 spike RBD

The 3D models of the spike RBD from the seven variants B.1.1.7 (known as alpha or UK variant), B.1.351 (known as beta or S. Africa variant), P1 (known as gamma or Japan/Brazil variant), B.1.617 (known as delta or India variant), B1.141 (detected for the first time in Scotland), B1.620 (detected for the first time in Cameroon); B.1.427 (known as California variant) were built by in silico mutagenesis of the Wuhan crystallized RBD, by using PyMOL 2.5.4, according to our validated protocols.[2,3]

More in detail, mutagenesis of the SARS-CoV-2 spike RBD was performed by using as a protein template the spike RBD extracted from the SARS-CoV-2 spike RBD/ACE2 protein complex (6m0j.pdb,[42]) hosting a complete RBD from the SARS-CoV-2 spike protein according to the Wuhan sequence (refseq_protein accession number YP_009724390.1) in complex with the human ACE2 receptor. The in silico mutagenesis tool implemented in PyMOL was used to introduce in the RBD object from 6m0j.pdb a group of missense mutations considered to play a crucial role in transmissibility/virulence in seven out of nine investigated variants, with specific reference to B.1.1.7 (with the analysed RBD mutations N501Y, S494P, E484K), B.1.351 (with the analysed RBD mutations K417N, E484K, N501Y), P1 (with the analysed RBD mutations K417T, E484K, N501Y), B.1.617 (with the analysed RBD mutations L452R; E484Q), B.1.141 (with the analysed RBD mutation N439K), B1.620 (with the analysed RBD mutations S477N, E484K), and B.1.427 (with the analysed RBD mutation L452R), as previously described.[2,3]

Due to the more recent spread of the Omicron subvariants, the structures of the RBD of the Omicron BA.1 (known as B.1.1.529, https://outbreak.info/situation-reports/BA.1; or https://cov-lineages.org/global_report_B.1.1.529.html, 7tl9.pdb[43]) and BA.4/5 (7xwa.pdb,[44] https://outbreak.info/situation-reports/BA.5) variants, crystallized in complex with the human ACE2 receptor, were included in our analyses for comparative purposes.

The RBD sequences from the investigated variants were downloaded from the PDB and aligned by using ClustalW[45] implemented in the Jalview package.[46]

Thus, the crystallized Wuhan spike RBD, used as a protein template for the comparative modeling session, the seven generated 3D models of the spike RBD from the cited seven investigated variants, and the two crystallized structures of the spike RBD from Omicron B.1.1.529 and BA.4/5 were minimized by using the Yasara minimization server and repaired by using the FoldX4 "repair" plug-in implemented in Yasara.[2,3,34,35,47,48] The Yasara minimization server performs energy minimization of protein models by running molecular dynamics simulations of models in explicit solvent, using a new partly knowledge-based all-atom force field derived from Amber, whose parameters have been optimized to minimize the damage done to protein crystal structures according to previously described protocols.[48] The FoldX4 "repair" plug-in is used to identify those

residues that exhibit bad torsion angles, or Van der Waals' clashes in the protein structures, in order to solve all the detected protein structure problems. This is accomplished through a small optimization process, in which the problematic residues and their neighbors are mutated to themselves, while exploring different rotamer combinations to find new energy minima, preventing residues from assuming bad torsion angles, or causing Van der Waals' clashes.[47]

2.2 | Analysis of the Omicron spike RBD/ACE2 protein complexes

The structures of the Omicron spike RBD from BA.1 (also known as B.1.1.529) and BA.4/5 subvariants crystallized in complex with the human ACE2 were downloaded from the protein data bank (7t9l.pdb,[43] and 7xwa.pdb,[44] respectively) and minimized by using he Yasara minimization server. The minimized structures were refined by using the FoldX "repair" plug-in implemented in Yasara by using the repair tool of FoldX. The interaction energy at the spike RBD/ACE2 protein–protein interface was calculated as above described for RBD/ab or RBD/nb protein complexes, according to.[2,3]

2.3 | Selection of ab and nb for the estimation of the spike RBD/ab or spike RBD/nb binding affinity

For the analysis of the interactions between the spike RBD of the investigated variants and ab/nb, we selected 14 ab and 5 nb. A total of 3 out of the 14 ab have been employed in clinical trials, with specific reference to the REGN10933 (6xdg.pdb), REGN10987 (6xdg.pdb,[15]) (https://clinicaltrials.gov/ct2/show/NCT04666441), and LY-CoV555 (7kmg.pdb,[26]) (https://clinicaltrials.gov/ct2/show/NCT04427501). Furthermore, 5 out of the 14 ab, namely CT-P59 (7cm4.pdb,[16]), CV503 (7lq7.pdb,[30]), COVA1.16 (7lq7.pdb)[30]), LY-CoV481 (7kmi.pdb), and LY-CoV488 (7kmh.pdb), were isolated from COVID-19 convalescent patients,[49] and considered here for the analysis of interactions.[2,3]

In addition, the ab CR3022 and m396 isolated from two SARS-CoV-1 convalescent patients and crystallized in complex with SARS-CoV-1 spike RBD (m396; 2dd8.pdb,[28]) or with both SARS-CoV-1 spike RBD (CR3022; 7jn5.pdb,[29]) and SARS-CoV-2 spike RBD (CR3022; 6zh9.pdb,[25]), whose binding affinities for the Wuhan SARS-CoV-2 spike RBD, were estimated in our previous work,[2] have also been included in our analyses for comparative purposes. Finally, the recently proposed humanized ab ADG20 (7u2d.pdb,[31]) was included in our analysis, being ADG20 a monoclonal ab advancing through global clinical trials proposed to provide durable protection against COVID-19 also related to the latest variants, for up to 1 year.

The first 4 nb selected for our analysis are represented by Ty1 (6zxn.pdb),[17] H11-H4 (6zh9.pdb),[25] VHH_U (7kn5.pdb), and VHH_E (7kn5.pdb).[27]

Following the recent crystallization of the Omicron spike RBD in complex with ab and nb, we considered in our analysis also 3 ab and 1 nb crystallized in complex with the spike RBD from Omicron BA.1 (namely 7qnw.pdb,[33] hosting the C1 nb and the Beta27 ab), and Omicron BA.4/5 (7zxu.pdb,[32] hosting the Beta-55 and EY6A ab).

The sequences of the investigated crystallized ab and nb proteins were downloaded from the PDB and aligned by using ClustalW.[45] The obtained alignment was checked and optimized by visual inspection.[50]

2.4 | Preparation of 3D protein complexes hosting the investigated ab/nb and the spike RBD from the investigated variants

To build the protein complexes hosting the investigated ab/nb interacting with the 3D comparative models of the spike RBD from the investigated variants, the RBD domain of the available cited crystallized SARS-CoV-2 spike RBD/ab or RBD/nb protein complexes was structurally aligned to the minimized/repaired RBD of the Wuhan spike protein extracted from 6m0j.pdb by using the "align/super" commands implemented in PyMOL 2.5.4 (according to validated protocols[2,3,34,35]).

Similarly, the modeled spike RBD domain of the cited seven investigated variants (minimized/repaired as above described starting from the spike RBD of 6m0j.pdb) and the two Omicron spike RBD crystallized structures were also structurally aligned to the RBD of the Wuhan spike protein extracted from 6m0j.pdb by using the "align/super" commands implemented in PyMOL 2.5.4 (according to validated protocols[2,3,34,35]).

As all the structural alignments were obtained for each investigated ab/nb, a new object hosting the atomic coordinates of the investigated ab/nb and the minimized/repaired Wuhan spike RBD domain (energetically minimized/repaired as above described starting from 6m0j.pdb) was generated. Similarly, a new object hosting the atomic coordinates of the investigated ab/nb and the minimized repaired Omicron spike RBD domains (energetically minimized/repaired as above described starting from 7t9l.pdb or 7wxa.pdb), or the 3D models of the other seven investigated variants (energetically minimized/repaired as above described), was also generated. In total 190 protein complexes (19 ab/nb multiplied for 10 variants, see also Supporting Information Materials for technical details about the choice of the chains to be modeled/used, within multichain crystallized protein complexes, for interaction energy calculations) were generated for the following interaction energy analysis.

It was chosen to align the generated spike RBD models from the cited variants and the spike RBD from the investigated crystallized RBD/ab or RBD/nb protein complexes with the RBD of 6m0j.pdb, before saving the new object hosting the RBD of the investigated variants in complex with the investigated ab/nb. The new objects were built by the cited superimposition operations for creating a unique molecular framework for allowing a quick comparative analysis of the interaction network established in the generated 3D protein complexes by using the spike RBD from 6m0j.pdb as a

reference structure.[2,3] In addition, the employment of the RBD from 6m0j.pdb allows comparing the results of the presented analyses with those previously obtained.[2,3]

2.5 | Structural analysis for verifying the abilities of the investigated ab/nb in targeting more than one RBD on the entire Wuhan trimeric spike protein without creating clashes

Protein complexes hosting the entire trimeric spike protein in different conformations, interacting simultaneously with three nb or with three ab (FAB portions) were obtained by creating three replicated objects of the investigated RBD/ab or RBD/nb protein complexes and by structural aligning the RBD of the replicated objects, for each investigated RBD/ab or RBD/nb protein complexes, with the three RBD on the entire trimeric spike protein structure available in four main different states in the PDB. The trimeric spike protein conformations used for performing the structural alignment and/or superposition operations were 6xm5.pdb, corresponding to the trimeric spike state with the 3 RBD in down-conformation, 7kmz.pdb, corresponding to the trimeric spike state with 2 RBD in up and 1 RBD in down-conformation, 7kms.pdb, corresponding to the trimeric spike state with 3 RBD in up-conformation, and 6zxn.pdb, corresponding to the trimeric spike state with 2 RBD in down- and 1 RBD in up-conformation.

As all the structural alignments were obtained, a new object hosting the atomic coordinates of the investigated ab/nb and the entire trimeric spike protein in the four investigated conformations was generated, producing 76 protein complexes (19 ab/nb multiplied for the investigated 4 conformations of the trimeric spike protein, see also Supporting Information Materials for technical details about the choice of the chains to be modeled/used, within multichain crystallized protein complexes, for interaction energy calculations).

2.6 | Derivation of putative nb from the investigated ab

Starting from the previously generated 76 protein complexes, new putative nb were obtained from the FAB portions of the investigated ab for investigating their abilities in targeting more than one RBD on the trimeric spike protein without creating the clashes observed in the presence of the entire FAB portion. To obtain the proposed nb from the FAB portions of the investigated ab, the heavy chains of the investigated ab (i.e., from the FAB portions available on the PDB) were cut at the level of residue T123 (according to REGN10933 sequence numbering, from 6xdg.pdb, see the provided alignment in the Results section).

Thus, a new object hosting the atomic coordinates of the investigated nb and/or derived-nb and the entire trimeric spike protein in the four investigated conformations was generated, producing 76 protein complexes (19 nb/derived-nb multiplied for the investigated 4 conformations of the trimeric spike protein, see also Supporting Information Materials for technical details about the choice of the chains to be modeled/used, within multichain crystallized protein complexes, for interaction energy calculations).

2.7 | Interaction energy calculations

All the 190 generated 3D all-atom protein complex models (obtained as described in the flow chart of Figure 1, see also Supporting Information Materials for technical details about the choice of the chains to be modeled/used, within multichain crystallized protein complexes, for interaction energy calculations) hosting the spike RBD in complex with the investigated nb or with the FAB portions of the investigated ab, were energetically minimized using the Yasara minimization server and residues packing was checked and repaired according to the FoldX repair function.[48] Similarly, the four 3D all-atom protein complex models (obtained as described in the flow chart of Figure 2) hosting the nb, the FAB portions of the investigated ab, or the corresponding derived nb, in complex with the three RBD of the entire trimeric spike protein, were energetically minimized by using the Yasara minimization server, if those protein complexes did not show clashes. PyMol 2.5.4[51] (https://www.pymol.org) was then used for examining (by visual inspection) the obtained 3D structure models, and for checking the correct packing of local secondary structures, according to our validated protocols.[2,3,34,35,50,52–54]

The interaction energy at the spike RBD/ab or RBD/nb or RBD/derived nb protein–protein interface in the minimized/repaired 3D models for all the cited generated protein complexes (according to Figures 1 and 2) was calculated by using FoldX4 and the FoldX Analyse Complex assay,[47] according to validated protocols.[2,3] More in detail, the FoldX Analyse Complex operates by unfolding the selected targets and by determining the stability of the remaining molecules. Then it subtracts the sum of the individual energies from the estimated global energy. More negative energies indicate a better binding, whereas positive energies indicate no binding.[47,55]

3 | RESULTS

3.1 | Multiple sequence alignment of the spike RBD from the investigated variants and of the investigated ab/nb

The analysis about the spread of SARS-CoV-2 variants in the last years has highlighted the important role played by amino acid replacements occurring at the spike RBD in variants escape from ab or nb recognition.[2,56] Amino acid replacements occurring at the spike RBD, investigated in this manuscript, are reported in Figure 3. Recently, we have presented a pipeline for calculating the interaction energy at the VoC spike RBD/ACE2 protein-protein interface, which may provide clues about transmissibility and/or virulence of new variants.[2,3,57–59] Here we present an adaptation/implementation of our computational

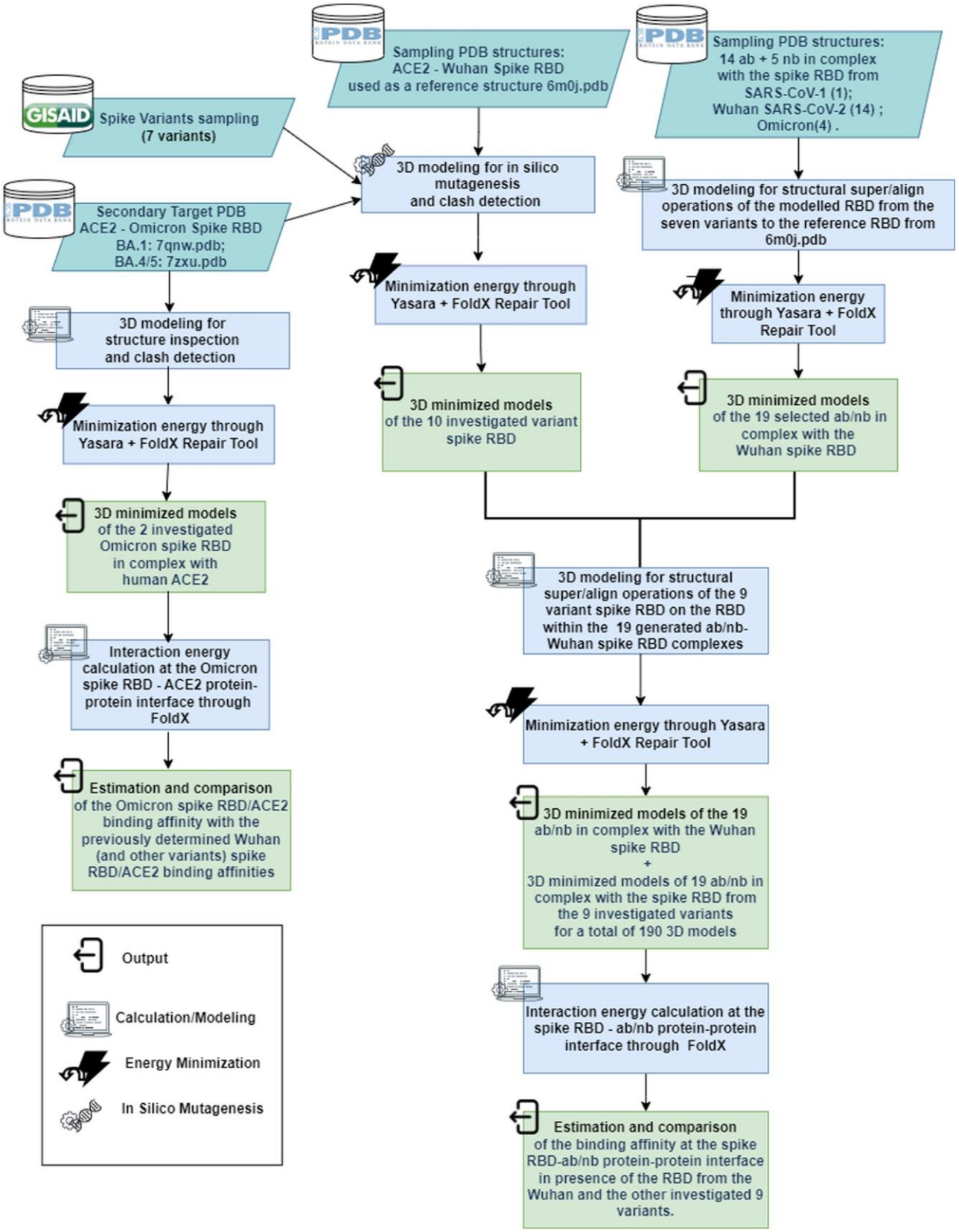

FIGURE 1 The flow chart describes a possible strategy to investigate spike RBD/ACE2 or spike RBD/ab or spike RBD/nb protein–protein interactions. The main goal of the flow chart (the estimation and comparison of protein–protein binding affinity) is reported in the last rectangle of each reported pipeline. ab, antibodies; ACE2, angiotensin converting enzyme 2; nb, nanobodies; RBD, receptor binding domain.

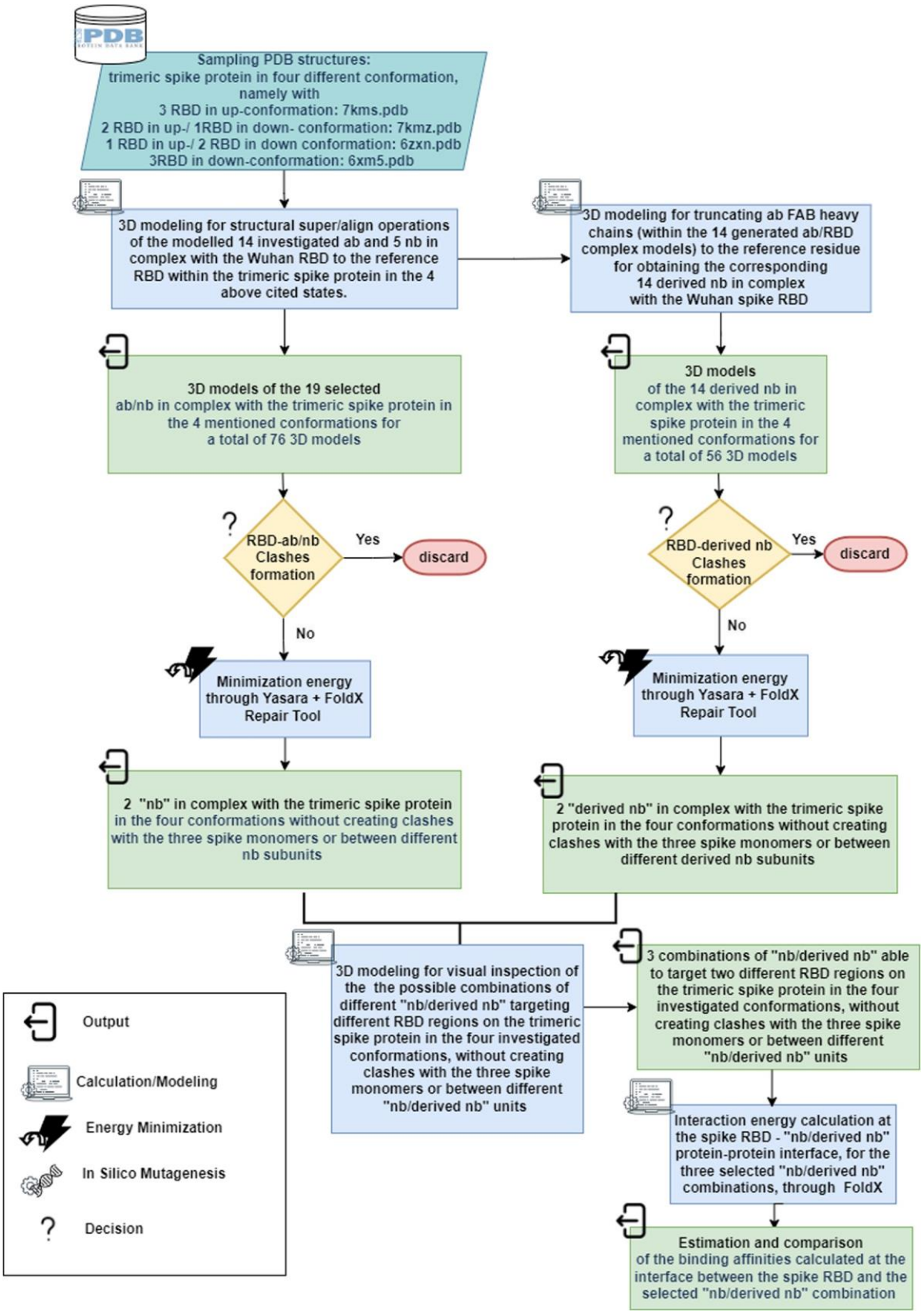

FIGURE 2 The flow chart describes a possible strategy to investigate spike RBD/ab or spike RBD/nb or spike RBD/derived-nb protein-protein interactions. The main goal of the flow chart (the estimation and comparison of protein–protein binding affinity) is reported in the last rectangle of the reported pipeline. ab, antibodies; ACE2, angiotensin converting enzyme 2; nb, nanobodies; RBD, receptor binding domain.

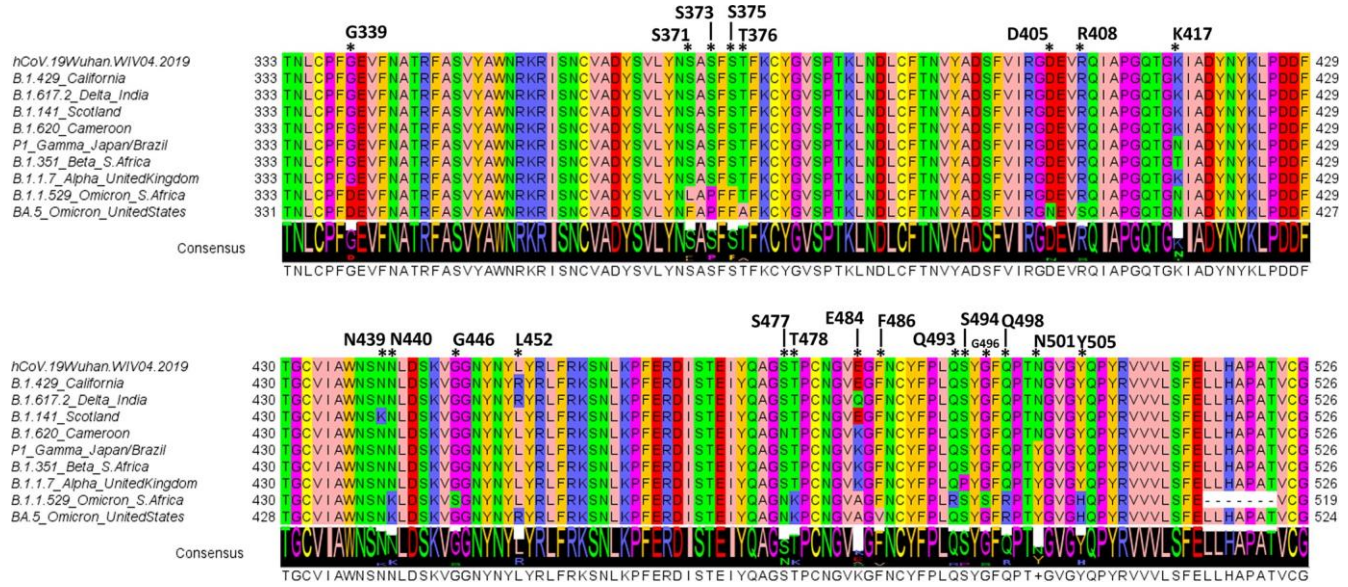

FIGURE 3 Multiple sequence alignment (MSA) of SARS-CoV-2 spike RBD sequences highlighted from the indicated sequenced variants. The MSA of the SARS-CoV-2 spike RBD from 6m0j.pdb (according to the Wuhan YP_009724390.1 sequence, used as a reference sequence) and the spike RBD, as sequenced from the cited variants, are reported in the figure. Amino acid replacements observed at the investigated RBD positions K417; N439; L452, S477, E484; S494; N501, in the first investigated variants, together with the 15 new mutations observed in Omicron subvariants at position G339, S371, S373, S375, T376, D405, R408, N440, G446, T478, F486, Q493, G496, Q498, Y505 (according to the Wuhan YP_009724390.1 sequence residues numbering) are indicated by a "*" symbol and labeled. Notably, five out of the first six amino acid positions involved in mutations (i.e., K417, L452, S477, E484, N501) were found mutated also in Omicron subvariants. The sequences of the SARS-CoV-2 spike RBD from Omicron B.1.1.529 variant also show a seven amino acid deletion. The MSA of the reported spike RBD sequences was obtained by ClustalW implemented in JalView. The MSA is colored according to the JalView Zappo style (green: hydrophilic residues (N, S, Q, T); salmon: aliphatic/hydrophobic residues (V, I, L, A); orange aromatic residues (Y, F, W); yellow: cysteine residues; magenta: conformationally special residues (P, G); red: acidic negative residues (D, E); blue: basic positive residues (R, K), i.e., see: https://www.jalview.org/help/html/colourSchemes/zappo.html). RBD, receptor binding domain; SARS-CoV-2, severe acute respiratory syndrome coronavirus 2.

pipeline for the estimation of the interaction energy at the "SARS-CoV-2 spike RBD/ab" or "RBD/nb" protein–protein interface for all the investigated SARS-CoV-2 spike RBD/ab or RBD/nb crystallized/modeled pairs (Figures 3 and 4, Table 1).

The alignment of the investigated ab or nb is reported in Figure 4. The color variation of residues within the ab/nb complementary determining regions (CDR1-3) indicates the positionof the variable portions responsible for the different affinity of theanalysed ab/nb for the investigated spike RBD variants (Figure 4).

3.2 | Spike RBD regions targeted by the investigated ab/nb

The investigated ab/nb bind preferentially four different RBD regions on the boat-shaped RBD surface,[3] indicated in Figure 5A,B as "stern," "hull," "bow," and "rudder." It is observed that the seven residues involved in mutations observed after the sequencing of the investigated highly more transmissible variants, before the appearance of Omicron subvariants, locate at the highlighted regions at the interface with ACE2. I.e, S477 is located at the bow region, E484 is located between the bow and the hull region, S494 and L452 locate on the hull region, K417 locates on the hull* region, N501 locates on the stern* region, whereas N439 locates on the rudder* region. Remarkably, all the seven amino acids affected by mutations locate in regions deeply involved in direct interactions with the investigated ab/nb (Figure 5).

More in detail, it is observed that among the investigated ab or nb, m396 (2dd8.pdb,[28]), REGN10987 (6xdg.pdb,[15]), and ADG20 (7u2d.pdb,[31]) bind the stern/stern* portion of the boat-shaped spike RBD (Table 2 and Figure 5C). The ab Ly-CoV488 (7kmh.pdb,[26]), Ly-CoV481 (7kmi.pdb,[26]), CT-P59 (7cm4.pdb,[16]), and the nb VHH_E (7kn5.pdb),[27] ab Ly-CoV555 (7kmg.pdb,[26]), and nb Ty1 (6zxn.pdb),[17] and H11-H4 (6zh9.pdb),[25] bind the hull/hull* portion of the boat-shaped spike RBD (Table 2 and Figure 5D). The ab CV503 (7lq7.pdb,[30]) and REGN10933 (6xdg.pdb,[15]) bind the bow portion (Figure 5); whereas COVA1.16 (7lq7.pdb,[30]), the nb VHH_U (7kn5.pdb,[27]) and CR3022 (6zh9.pdb,[25]) bind the rudder portion (Figure 5E).

3.3 | Spike RBD sequences and ab/nb related to the Omicron variant and interaction energy at the Omicron spike RBD/ACE2 protein–protein interface

The RBD of the spike proteins of the SARS-CoV-2 Omicron B.1.1.529 (also known as BA.1, 7tl9.pdb) and BA.4/5 (7xwa.pdb) variants present

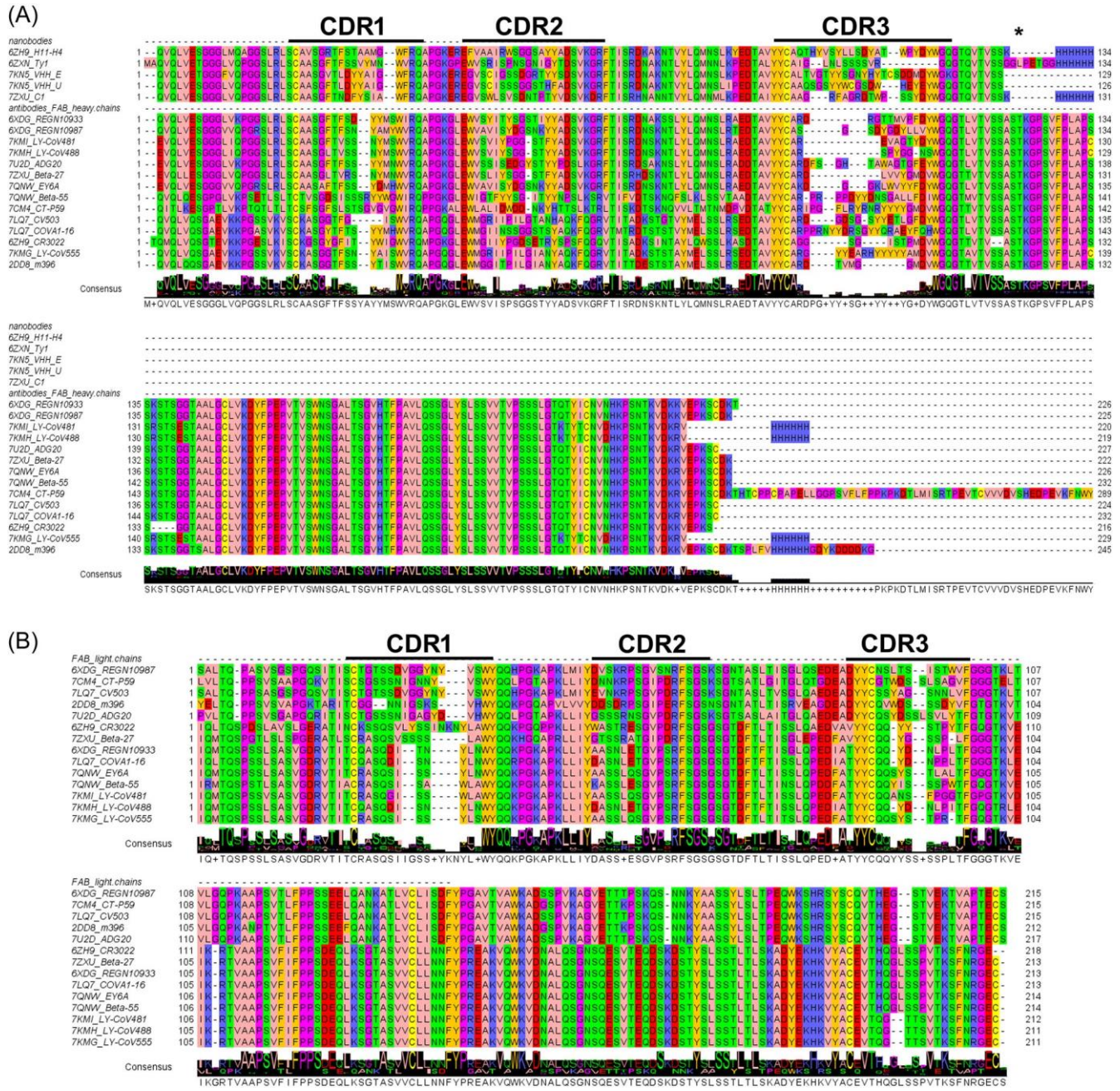

FIGURE 4 Protein sequence alignment of the investigated crystallized ab, namely heavy chains of the FAB, and nb in (A); light chains of the ab FAB portions in (B). Black lines indicate the localization of complementary determining regions (CDR1-3) on the investigated ab/nb involved in the recognition/binding of the spike RBD. The "*" symbol indicates the position (i.e., T123 with reference to REGN10933 heavy chain sequence numbering) at which the investigated ab heavy chains were truncated for deriving the proposed nb as they would be obtained starting from the investigated ab for the analysis related to the ab/nb cocktails (see Section 3.7). The MSA is colored according to the JalView Zappo style (green: hydrophilic residues (N, S, Q, T); salmon: aliphatic/hydrophobic residues (V, I, L, A); orange aromatic residues (Y, F, W); yellow: cysteine residues; magenta: conformationally special residues (P, G); red: acidic negative residues (D, E); blue: basic positive residues (R, K), i.e., see: http://www.jalview.org/help/html/colourSchemes/zappo.html). ab, antibodies; nb, nanobodies; RBD, receptor binding domain; SARS-CoV-2, severe acute respiratory syndrome coronavirus 2.

15 and 16 mutations at variance with the RBD of the Wuhan spike sequence. Remarkably, BA.4 and BA.5 variants show the same mutations at the spike RBD.[32] A total of 11 out of the 15 mutations in the spike protein from SARS-CoV-2 Omicron B.1.1.529 and 11 out of the 16 mutations in the spike protein from SARS-CoV-2 Omicron BA.4/5 are in amino acid positions not mutated in the RBD of the spike protein of previously described variants (Table 2).

In addition, B.1.1.529 shows a deletion of seven amino acids between residues E516-V524 (Wuhan sequence numbering, see Figure 3).[32] All the described mutations locate on the described

TABLE 1 List of the investigated ab/nb crystallized in complex with the spike RBD.

ab/nb	PDB_ID	Variant targeted domain	Targeted RBD area	Method	Resolution (Å)
m396	2dd8	SARS-CoV-1 spike RBD	stern*	X-ray diffraction	2.30
ADG20	7u2d	Wuhan SARS-CoV-2 spike RBD		X-ray diffraction	2.76
beta55	7qnw	Omicron B.1.1.529 spike RBD		X-ray diffraction	2.40
REGN10987	6xdg	Wuhan SARS-CoV-2 spike RBD	stern	electron microscopy	3.90
H11-H4 (nb)	6zh9	Wuhan SARS-CoV-2 spike RBD	hull	X-ray diffraction	3.31
Ty1 (nb)	6zxn	Wuhan SARS-CoV-2 trimeric spike protein		electron microscopy	2.93
CT-P59	7cm4	Wuhan SARS-CoV-2 spike RBD		X-ray diffraction	2.71
VHH_E (nb)	7kn5	Wuhan SARS-CoV-2 spike RBD		X-ray diffraction	1.87
Ly-CoV555	7kmg	Wuhan SARS-CoV-2 spike RBD		X-ray diffraction	2.16
Ly-CoV488	7kmh	Wuhan SARS-CoV-2 spike RBD	hull*	X-ray diffraction	1.72
Ly-CoV481	7kmi	Wuhan SARS-CoV-2 spike RBD		X-ray diffraction	1.73
beta27	7zxu	Omicron BA.4/5 spike RBD		X-ray diffraction	1.89
CV503	7lq7	Wuhan SARS-CoV-2 spike RBD	bow	X-ray diffraction	3.40
REGN10933	6xdg	Wuhan SARS-CoV-2 spike RBD		electron microscopy	3.90
CR3022	6zh9	Wuhan SARS-CoV-2 spike RBD	rudder*	X-ray diffraction	3.31
VHH_U (nb)	7kn5	Wuhan SARS-CoV-2 spike RBD		X-ray diffraction	1.87
CoVa1.16	7lq7	Wuhan SARS-CoV-2 spike RBD		X-ray diffraction	3.40
EY6A	7qnw_	Omicron B.1.1.529 spike RBD		X-ray diffraction	2.40
C1 (nb)	7zxu	Omicron BA.4/5 spike RBD		X-ray diffraction	1.89

Note: The reported ab/nb are crystallized in complex with the RBD of the Wuhan SARS-CoV-2 spike protein, with the exception of the ab m396, crystallized in complex with the RBD of the SARS-CoV-1 spike protein, the ab Beta55 and EY6A crystallized in complex with the RBD of the SARS-CoV-2 Omicron-B.1.1.529 variant, and the ab Beta27 and the nb C1 crystallized in complex with the spike RBD of SARS-CoV-2 Omicron BA.4/5 variant. For an explanation of the "*" symbol, see Figure 5 and the related figure legend.

Abbreviations: ab, antibodies; nb, nanobodies; RBD, receptor binding domain.

regions highlighted on the dashed boat-shaped RBD surface (Table 2, Figures 5A and 6A).

More in detail, in our analysis we proposed to divide the characterized mutations and the new mutations by considering S477, T478, F486, and E484 as part of the bow region, Q493,S494, D405, R408, K417, L452 as part of the hull/hull*, N439, N440, G446, G496, Q498, N501, Y505 as part of the stern/stern*, and G339, S371, S373, S375, T376 as participating to the rudder/ rudder* region. The high number of new mutations conferred to Omicron variant and subvariants very high transmissibility.[60] According to our computational pipeline, the estimated interaction energy at the Omicron spike RBD/ACE2 protein–protein interface was less negative (reflecting a lower affinity) than its counterpart estimated for previous variants (i.e., the interaction energy at the spike RBD/ACE2 protein-protein interface was −20.51 kcal/mol for the Wuhan variant, or −21.37 kcal/mol for the P1.Japan/Brazil variant) (Table 3).[3]

Conversely, the overall surface of interaction with ACE2 was unchanged. Indeed, the root mean square deviation between atomic coordinates of the Wuhan SARS-CoV-2 spike RBD/ACE2 (6m0j.pdb) and the Omicron B.1.1.529 SARS-CoV-2 spike/ACE2 (7t9l.pdb,[43]) protein complexes is 0.5 Å (Figure 6B), despite of the high number of amino acids undergoing mutations in the omicron variant, observed on the boat-shaped surface of the spike RBD (Figure 6).

Remarkably, also the targeted regions of ab/nb directed against the RBD of the Omicron spike variants remained the same, as observed in the solved crystallized structures of the SARS-CoV-2 Omicron spike variants in complex with the nb C1 and the ab Beta-27 (7zxu.pdb,[32]), which target a region close to the rudder* (CDRs pointing mainly towards S373, S375, T376, R408), and the hull* (CDRs pointing mainly towards K417, Q493) binding region, respectively, of the SARS-CoV-2 Omicron BA.5 spike RBD, or the Ab Beta-55 and EY6A (7qnw.pdb,[33]) targeting the stern* (CDRs pointing mainly towards N439, N440) and rudder* (CDRs pointing mainly towards a region below S373, S375, T376, R408, being the closest residue T385) binding regions, respectively, of the SARS-CoV-2 Omicron B.1.1.529 spike RBD (Figure 6).

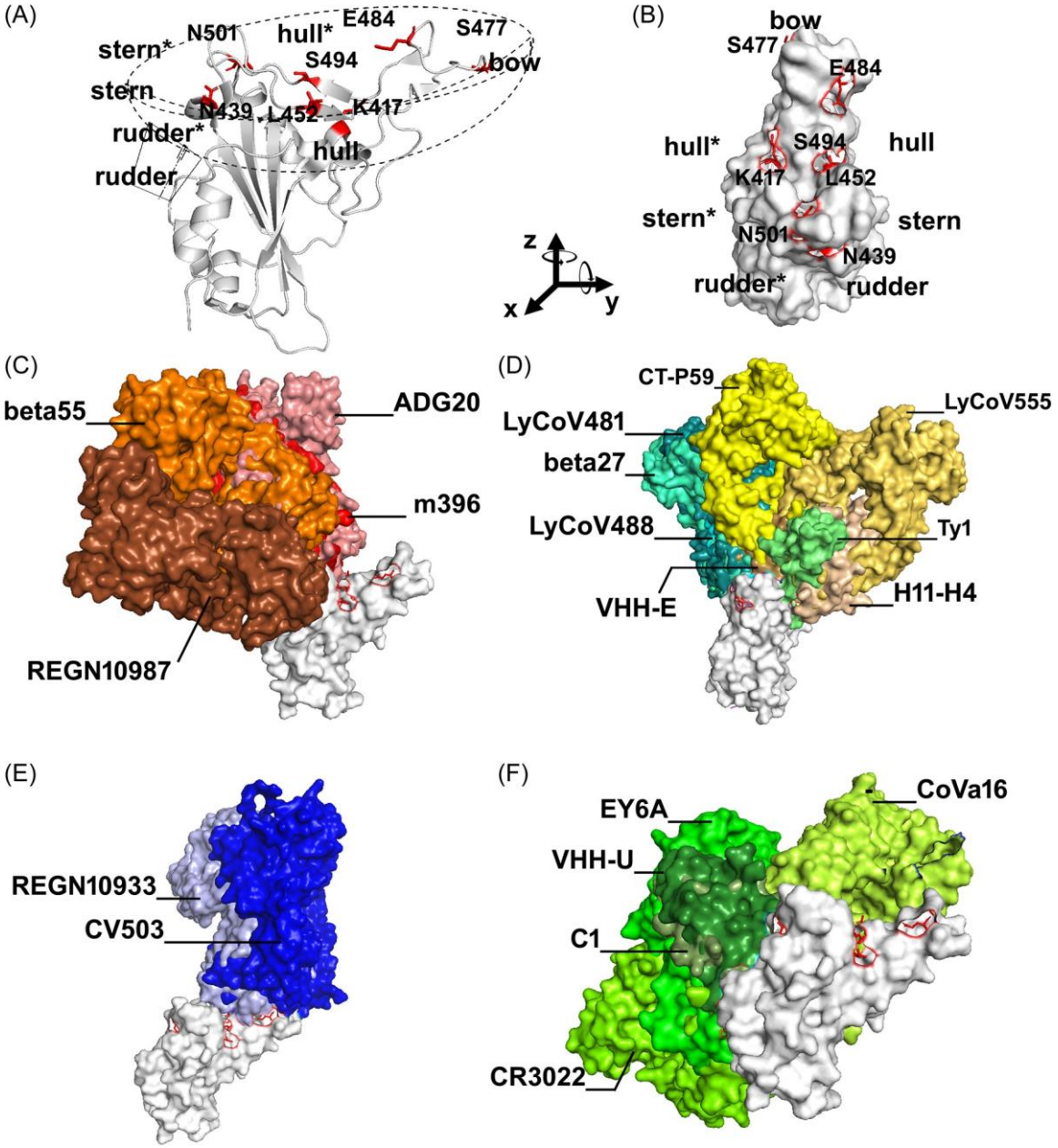

FIGURE 5 Structure of the SARS-CoV2 spike RBD in complex with the investigated nb or with the FAB portions of the investigated ab targeting four main regions of the RBD, as highlighted by the crystallized structures, whose PDB_IDs are listed in Table 1. The four regions, being located on the boat-shaped surface of the RBD (according to Tragni et al.[3]) indicated by the dashed line, are called bow, stern, hull, and rudder. The presence of the "*" symbol indicates that the targeted region is on the left side of the boat-shaped area [i.e., closer to the protein region hosting K417, according to the views reported in (B)], whereas the absence of "*" indicates that the target region is on the right side of the boat-shaped area [i.e., closer to the protein region hosting L452, according to the views reported in (B)].
(A) Lateral view of the boat-shaped spike RBD highlighting the six different spike RBD regions (indicated as stern, stern*, bow, hull, hull*, rudder, and rudder*). (B) The top view of the spike RBD obtained by anticlockwise rotation of approximately 90 degrees, along the z- and y-axis. of the RBD depicted in (A), is reported in surf white representation. The seven amino acid positions involved in mutations in the most famous variants, before the appearance of Omicron variants, are reported in red sticks. Ab or nb mainly targeting residues on the stern/stern* portion (C), the hull/hull* portion (D), the bow portion (E), and the rudder* portion, respectively, of the boat-shaped RBD surface (in white surf representation) are reported in colored surf representation and labeled. ab, antibodies; nb, nanobodies; RBD, receptor binding domain; SARS-CoV-2, severe acute respiratory syndrome coronavirus 2.

TABLE 2 List of variants and the investigated missense mutations detected at the RBD (see also Figure 3).

VoC/VoI pangolin name/WHO/main diffusion region	B.1.1.529 Omicron South Africa	BA.4/5 Omicron South Africa	B.1.1.7 Alpha United Kingdom	B.1.351 Beta South Africa	P.1 Gamma Brazil/ Japan	B.1.617.2 Delta India	B.1.429 California	B.1.141 Scotland	B.1.620 Cameroon
RBD amino acid positions involved in mutations			E484, S494, N501	K417, E484, N501	K417, E484, N501	L452, E484	L452	N439	S477, E484
RBD missense mutations observed with respect to the Wuhan spike RBD sequence	G339D	G339D							
	S371L	S371F							
	S373P	S373P							
	S375F	S375F							
		T376A							
		D405N							
		R408S							
	K417N	K417N		K417N	K417T				
								N439K	
	N440K	N440K							
	G446S								
		L452R				L452R	L452R		
	S477N	S477N							S477N
	T478K	T478K							
	E484A	E484A	E484K	E484K	E484K	E484Q			E484K
		F486V							
	Q493R								
			S494P						
	G496S								
	Q498R	.							
	N501Y	N501Y	N501Y	N501Y	N501Y				
	Y505H	Y505H							

Note: In the first row of the table the available variant designations are reported according to https://cov-lineages.org/lineage_list.html. In the second row of the table the Pangolin nomenclature is reported, with the proposed first geographic appearance/localization of the reported variants. The names and numbers of the missense mutations detected at the RBD of the investigated variants are reported by using the amino acid one-letter code. For a complete list of designations of current and withdrawn variants visit https://github.com/cov-lineages/pango-designation/blob/master/lineage_notes.txt.

Abbreviations: RBD, receptor binding domain; WHO, World Health Organization.

3.4 | Calculation of the interaction energy at the protein–protein interface in the protein complexes hosting the spike RBD of the 10 investigated variants and the investigated 14 ab and 5 nb

To investigate how the replacement of the 7 (prior to the appearance of Omicron) to 22 (after Omicron) investigated RBD residues determines a variation of the RBD/ab or RBD/nb binding affinities,[3] the interaction energy at the RBD/ab or RBD/nb protein-protein interface for the cited 14 antibodies and 5 nanobodies was calculated by using the FoldX4 software implemented in the Yasara package, as previously described.[2,3,47,48] From the performed analysis, we observed that the ab Beta27 and Ly-CoV488 targeting the RBD hull*/hull regions resulted in the RBD/ab complexes with the lowest free energy of binding (i.e., forming the most stable interactions), as calculated by FoldX4. More in general, the performed analysis shows that ab/nb directed against the hull* region are those involved in stronger interactions with the spike RBD, whereas ab directed against the stern/stern* spike RBD portions form weaker interactions with the spike RBD, at least in presence of the ab/nb analysed in this study (Figure 7).

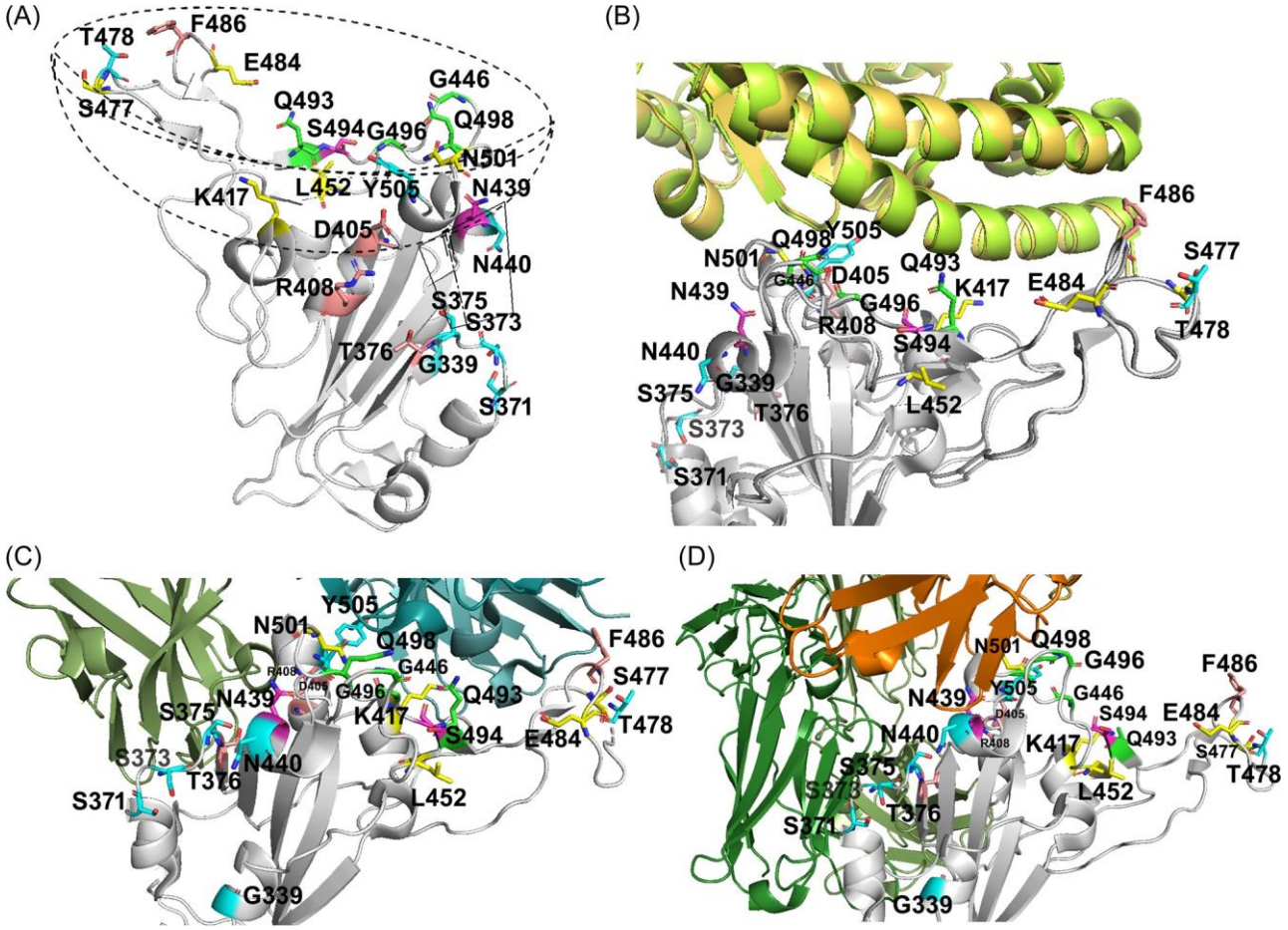

FI GURE 6 Localization of SARS-CoV-2 spike RBD positions undergoing mutations in the investigated variants, including the analysed Omicron variants, with respect to ACE2 and the crystallized investigated ab/nb. (A) Amino acid positions concerning residues observed mutated both in B.1.1.529 and BA.4/5, never observed mutated in previously cited variants, are reported in cyan sticks (7 residues, G339, S371, S373, S375, N440, T478, Y505). Amino acid positions concerning residues observed mutated only in BA.4/5 or in B.1.1.529, never found mutated in the previously cited variants are reported in salmon (4 residues, T376, D405, R408, F486) or green (4 residues, G446, Q493, G496, Q498) sticks, respectively. Amino acid positions concerning residues found mutated in at least one Omicron subvariant, already found mutated in the previously described variants, are reported in yellow sticks (5 residues, K417, L452, S477, E484, N501). Amino acid positions concerning residues found mutated in the previously cited variants, without being mutated in Omicron subvariants, are reported in magenta sticks (2 residues, N439, S494). The proposed RBD side view was chosen for allowing a better inspection/visualization of the highlighted residues undergoing mutations in the Omicron variants. The boat-shaped surface of the RBD (according to Tragni et al.[3]) is indicated by the black dashed line. (B) The superimposition of the crystallized SARS-CoV-2 spike RBD from the Wuhan variant (6m0j.pdb) and from the Omicron B.1.1.529 variant (7t9l.pdb) are reported in white and gray cartoon representation, respectively. Labels indicate the positions of amino acids undergoing missense mutations in the investigated variants, as highlighted in (A). ACE2 receptors domains from 6m0j.pdb (yellow-orange cartoon) and 7t9l.pdb (yellow-lemon cartoon) are reported for comparative purposes for highlighting the overall surface of interaction with the reported RBD domains. The proposed RBD side-view, rotated of 180° compared to the view reported in (A), was chosen for allowing a better visualization of the surface of interaction with ACE2. (C) The ab Beta27 in darkcyan cartoon and the nb C1 in smudge cartoon (taken from 7xzu.pdb) were crystallized in complex with the spike RBD of the SARS-CoV-2 Omicron BA.5 variant. In this figure the spike RBD of the SARS-CoV-2 Omicron BA.5 variant (taken from 7zxu.pdb) was superimposed (structurally aligned) to the RBD of 6m0j.pdb for creating the picture reported in (C) showing the "ab Beta27/nb C1" in complex with the spike RBD from the Wuhan variant (white cartoon) extracted from 6m0j.pdb. The original crystallized structure and the shown 3D model, after the minimization/repair process described in the methods section, were used to calculate the interaction energy at the spike RBD/Ab or at the spike RB/nb protein–protein interface. It is noticed that BA.4 and BA.5 Omicron subvariants have no differences in their spike protein sequences. (D) The ab Beta55 in orange cartoon and of ab EY6A in darkgreen cartoon (taken from 7qnw.pdb) were crystallized in complex with the spike RBD of the SARS-CoV-2 Omicron B.1.1.529 variant. In this figure, the spike RBD of the SARS-CoV-2 Omicron B.1.1.529 variant was superimposed (structurally aligned) to the spike RBD of 6m0j.pdb for creating the picture reported in (D) showing the "ab Beta55/ab EY6A" in complex with SARS-CoV-2 spike RBD from the Wuhan variant (white cartoon) extracted from 6m0j.pdb. The original crystallized structure and the shown 3D model after the minimization/repair process described in the methods section were used to calculate the interaction energy at the spike RBD/Ab protein–protein interface. In all the reported panels residues from the Wuhan spike RBD undergoing mutations in the investigated variants are highlighted by colored sticks (according to the Wuhan spike RBD sequence numbering, from 6m0j.pdb) and labeled. For a complete list of the missense mutations observed in the investigated variants see Table 2. ACE2, angiotensin converting enzyme 2; RBD, receptor binding domain; SARS-CoV-2, severe acute respiratory syndrome coronavirus 2.

Pdb	7t9l B.1.1.529 spike_RBD vs ACE2	7xwa BA.4/5 spike_RBD vs ACE2
ACE2 (chain)	A	A
spike RBD (chain)	D	B
Intraclashes group 1	8.6	23.8
Intraclashes group 2	24.6	5.3
Interaction energy (kcal/mol)	−18.5	−16.2
Backbone H-bond	−2.2	−4.3
Sidechain H-bond	−7.2	−10.7
Van der Waals	−15.6	−15.7
Electrostatics	−2.4	−1.0
Solvation polar	20.2	22.5
Solvation hydrophobic	−19.1	−18.8
Van der Waals clashes	0.2	1.3
entropy sidechain	7.0	8.8
entropy mainchain	0.9	1.9
torsional clash	0.2	0.1
backbone clash	2.7	2.5
helix dipole	−0.1	0.0
disulfide	0.0	0.0
electrostatic kon	−0.6	−0.2
energy ionization	0.1	0.1
Entropy complex	2.4	2.4
Number of residues	796	791
Interface residues	41	40

Note: Please, note that more negative "interaction energy" values, reported here in kcal/mol, indicate stronger binding interactions and thus higher binding affinity at the protein-protein interface of the indicated SARS-CoV-2 spike RBD/ACE2.[2,3,47,55] The energy terms and contributions are reported in kcal/mol according to FOLDX indications. Each energy term has a specific weight in the calculation of the interaction energy, according to the equations reported in.[2,3,47,55] The calculated energy terms and item names are reported in the first cell of each row (i.e., in the first column of the reported table), whereas items (protein names, chain-ID, or protein PDB accession codes) and the calculated energy terms are reported within columns 2–3. The energy terms and contributions are reported in kcal/mol according to FOLDX indications For a complete explanation of item names and energy terms, please, visit the link http://foldxsuite.crg.eu/command/AnalyseComplex. Interaction energies are also reported in kJ/mol (1 kcal = 4.184 kJ). For the BA.4/5 spike RBD/ACE protein complex, the heterodimer consisting of chains AB was reported in the table showing a binding affinity higher than the ones calculated for the heterodimer consisting of chains CD (−14.59 kcal/mol).
Abbreviations: ACE2, angiotensin converting enzyme 2; RBD, receptor binding domain.

3.5 | Ab/nb combinations against the 3 RBD in the context of the trimeric spike protein in different conformations

To identify nb and ab FAB portions able to bind the 3 RBD of a trimeric spike protein, while the spike assumes different conformations, without creating clashes, we built the related protein complexes hosting the entire trimeric spike protein interacting with three nb or with three ab (FAB portions), by superimposing the investigated RBD/ab or RBD/nb protein complexes to the available entire trimeric spike protein structures solved in four different conformations, as observed in 6xm5.pdb, showing the 3 RBD in down-conformation; 7kmz.pdb, showing 2 RBD in up and 1 RBD in down-conformation; 7kms.pdb, showing 3 RBD in up-conformation; 6zxn.pdb, showing 2 RBD in down- and 1 RBD in up-conformation. The performed analysis, revealed that none of the investigated ab was able to bind simultaneously the three RBD of the spike protein, independently on their conformation, although the generated protein complexes host only the FAB portions of the investigated ab (Figure 8).

Furthermore, most of the investigated ab FAB portions can bind just one RBD, only if the targeted RBD is in up-conformation. It also appears that the "stern" and the "rudder*" regions of the boat-shaped RBD surface, cannot be accessed at all by the investigated ab FAB portions, directed towards the "stern/rudder*" area, when the three RBD are all in down-conformation (Figure 8). A set of possible clashes at the protein-protein interface is shown in Figures S1 and S2 reporting the 3D models of the FAB portions of LyCoV555 (the ab from which we derived one of the best nb, see below) or with Beta27 (the ab with the highest binding affinity for the RBD, according to Figure 7) in complex with the entire SARS-CoV-2 trimeric spike protein.

Conversely, while it was expected that nb can perform better in binding RBD of the trimeric spike protein, due to their smaller size, only two nb out of the five investigated nb, namely H11-H4 and Ty1, were able to bind the three RBD of the spike protein, either when the three targeted RBD (i.e., the "hull" region of the boat-shaped RBD surface) are all in up- or when the three RBD are all in down-conformation (see Figure 8).

3.6 | Derived nb from the FAB portions of the investigated ab for creating combinations of nb/derived-nb able to target simultaneously more than one RBD on the Wuhan trimeric spike protein in the four investigated spike conformations

In light of the above-reported observations, and to gain clues about future nb able to target simultaneously the three RBD of the spike protein, independently on their up-/down-conformations, the heavy chains of the investigated ab (FAB portions) were truncated for deriving putative/ideal nb to establish new nb able to efficiently

Interactions energies (kcal/mol) at the RBD/ab or RBD/nb protein-protein interface grouped according to the highlighted target regions	stern*			stern	hull*			hull					bow		stern				
Variants (analysed mutations on the RBD)	m396 (2dd8, chains HL)	Beta55 (7qnw chains AB)	ADG20 (7u2d, chains HL)	REGN10987 (6xdg, chains AC)	LY-CoV481 (7kmi, chains AB)	LY-CoV488 (7kmh, chains AB)	Beta27 (7zxu, chains HL)	LY-CoV555 (7kmg, chains AB)	H11.H4 (6zh9, chain F)	Ty1 (6zxn, chain B)	VHH E (7kn5, chain C)	CT-P59 (7cm4, chains HL)	CV503 (7lq7, chains HL)	REGN10933 (6xdg, chains BD)	CoVa1-16 (7lq7, chains PQ)	VHH U (7kn5, chain E)	EY6A (7qnw, chains HL)	CR3022 (6zh9, chains HL)	C1 (7zxu, chain A)
Wuhan SARS-CoV-2 Spike	-10.1	-17.0	-13.0	-9.1	-18.2	-25.1	-26.1	-21.2	-17.2	-13.6	-18.9	-17.4	-10.1	-17.0	-14.6	-9.4	-15.2	-11.4	-11.4
B.1.1.7 Alpha United Kingdom (S494P_N501Y_E484K)	-13.0	-17.8	-11.7	-10.2	-17.4	-25.1	-24.7	-13.6	-10.4	-9.0	-18.2	-17.4	-12.4	-11.5	-10.6	-8.9	-13.0	-15.1	-10.3
B.1.141 Scotland (N439K)	-12.2	-13.8	-12.2	-6.3	-18.5	-18.7	-24.5	-17.9	-19.0	-13.6	-13.3	-16.8	-13.0	-10.0	-18.7	-10.0	-13.0	-14.2	-8.8
B.1.351 Beta South Africa (N501Y_E484K_K417T)	-11.4	-16.4	-11.7	-8.3	-19.0	-21.8	-24.0	-18.0	-11.0	-8.8	-12.5	-15.6	-11.7	-12.2	-12.6	-10.2	-11.5	-16.6	-10.4
B.1.429 California (L452R)	-14.0	-14.1	-10.5	-10.4	-16.1	-22.7	-23.3	-19.1	-16.0	-15.1	-17.5	-17.8	-12.7	-9.1	-13.0	-7.7	-11.3	-13.8	-9.0
B.1.617.2 Delta India (E484Q_L452R)	-9.5	-12.7	-8.2	-10.2	-18.3	-16.2	-22.6	-17.1	-12.8	-9.7	-14.4	-13.6	-11.0	-12.1	-13.9	-8.5	-7.9	-13.8	-10.7
B.1.620 Cameroon (S477N_E484K)	-11.2	-13.9	-4.8	-9.1	-14.1	-13.2	-14.6	-15.6	-10.9	-11.8	-14.0	-18.0	-9.2	-12.8	-11.9	-8.8	-15.2	-17.4	-10.1
P.1 Gamma Brasil/Japan (N501Y_E484K_K417N)	-12.5	-13.4	-8.4	-8.2	-20.4	-22.8	-25.9	-16.3	-9.3	-9.2	-15.1	-14.6	-13.3	-13.5	-13.3	-9.7	-13.9	-14.1	-6.8
B.1.1.529 Omicron South Africa	-8.6	-14.6	-13.7	-10.5	-17.4	-21.7	-24.3	-14.6	-13.1	-11.1	-14.0	-13.4	-12.0	-12.5	-15.6	-4.7	-16.5	-20.8	-11.4
BA.4/5 Omicron South Africa	-9.1	-10.5	-7.7	-8.7	-14.3	-18.4	-23.3	-18.3	-14.9	-8.8	-14.5	-12.4	-9.1	-13.5	-14.4	-11.4	-10.4	-13.6	-17.6

stronger interactions (lower free energy) — weaker interactions (higher free energy)

FIGURE 7 Heatmap of the interaction energies (Kcal/mol) at the SARS-CoV2 spike RBD/ab or RBD/nb protein/protein interface calculated by using the FoldX plug-in implemented in the Yasara package. The boxes of each RBD/Ab(nb) pair were colored and color gradient between red (more negative predicted free energy of interaction, reflecting stronger interactions) and green (higher predicted free energy of interaction, reflecting weaker interactions) indicates the strength of the binding interactions. ab, antibodies; nb, nanobodies; RBD, receptor binding domain; SARS-CoV-2, severe acute respiratory syndrome coronavirus 2.

			Nb and Ab (FAB portions) clashes with adjacent spike monomers												Nb and "derived nb" clashes with adjacent spike monomers											
			6xm5_3.down			6zxn_2.down/1.up			7kmz_2.up/1.down			7kms_3.up			6xm5_3.down			6zxn_2.down/ 1.up			7kmz_2.up/1.down			7kms_3.up		
Targeted RBD region	PDB_ID	RBD chain orientataion ab-nb names	1 down	2 down	3 down	1 up	2 down	3 down	1 down	2 up	3 up	1 up	2 up	3 up	1 down	2 down	3 down	1 up	2 down	3 down	1 down	2 up	3 up	1 up	2 up	3 up
stern*	2dd8	m396	✗	✗	✗	✗	✗	✗	✗	✓	✓	✓	✓	✓	✗	✗	✗	✓	✗	✗	✓	✓	✓	✓	✓	✓
	7u2d	ADG20	✗	✗	✗	✓	✗	✗	✗	✓	✓	✓	✓	✓	✗	✗	✗	✓	✗	✗	✓	✓	✓	✓	✓	✓
	7qnw	beta55	✗	✗	✗	✗	✗	✗	✓	✓	✓	✓	✓	✓	✗	✗	✗	✓	✓	✓	✓	✓	✓	✓	✓	✓
stern	6xdg	REGN10987	✗	✗	✗	✓	✓	✗	✓	✓	✓	✓	✓	✓	✓	✓	✓	✓	✓	✓	✓	✓	✓	✓	✓	✓
hull	6zh9	H11-H4 (nb)	✓	✓	✓	✓	✓	✓	✓	✓	✓	✓	✓	✓	✓	✓	✓	✓	✓	✓	✓	✓	✓	✓	✓	✓
	6zxn	Ty1 (nb)	✓	✓	✓	✓	✓	✓	✓	✓	✓	✓	✓	✓	✓	✓	✓	✓	✓	✓	✓	✓	✓	✓	✓	✓
	7cm4	CT-P59	✗	✗	✗	✓	✗	✗	✗	✓	✓	✓	✓	✓	✗	✗	✗	✓	✗	✗	✗	✓	✓	✓	✓	✓
	7kn5	Vhh.E (nb)	✓	✓	✓	✓	✓	✗	✗	✓	✓	✓	✓	✓	✓	✓	✓	✓	✓	✗	✗	✓	✓	✓	✓	✓
	7kmg	Ly-CoV555	✓	✓	✓	✓	✓	✗	✗	✓	✓	✓	✓	✓	✓	✓	✓	✓	✓	✓	✓	✓	✓	✓	✓	✓
hull*	7kmh	Ly-CoV488	✗	✗	✗	✓	✗	✗	✗	✓	✓	✓	✓	✓	✗	✗	✗	✓	✗	✗	✗	✓	✓	✓	✓	✓
	7kmi	Ly-CoV481	✗	✗	✗	✓	✗	✗	✗	✓	✓	✓	✓	✓	✗	✗	✗	✓	✗	✗	✗	✓	✓	✓	✓	✓
	7zxu	Beta27	✗	✗	✗	✓	✗	✗	✗	✓	✓	✓	✓	✓	✗	✗	✗	✓	✗	✗	✗	✓	✓	✓	✓	✓
bow	7lq7	CV503	✓	✓	✓	✓	✓	✗	✗	✓	✓	✓	✓	✓	✓	✓	✓	✓	✓	✗	✗	✓	✓	✓	✓	✓
	6xdg	REGN10933	✗	✗	✗	✓	✗	✗	✗	✓	✓	✓	✓	✓	✗	✗	✗	✓	✗	✗	✗	✓	✓	✓	✓	✓
rudder*	6zh9	CR3022	✗	✗	✗	✗	✗	✗	✗	✗	✗	✗	✗	✗	✗	✗	✗	✗	✗	✗	✗	✗	✗	✓	✓	✓
	7kn5	Vhh.U (nb)	✗	✗	✗	✗	✗	✗	✗	✗	✓	✓	✓	✓	✗	✗	✗	✗	✗	✗	✗	✗	✓	✓	✓	✓
	7lq7	CoVa1.16	✗	✗	✗	✗	✗	✗	✗	✗	✓	✗	✗	✗	✗	✗	✗	✗	✗	✗	✗	✗	✗	✗	✗	✗
	7qnw	EY6A	✗	✗	✗	✓	✗	✗	✗	✗	✗	✗	✗	✗	✗	✗	✗	✗	✗	✗	✗	✗	✓	✓	✓	✓
	7zxu	C1 (nb)	✗	✗	✗	✗	✗	✗	✗	✗	✓	✓	✓	✓	✗	✗	✗	✗	✗	✗	✗	✗	✓	✓	✓	✓

FIGURE 8 The ability of the investigated ab/nb (or derived nb) in targeting one out of three RBD in the four main different conformations adopted by the three RBD within the (full-length) trimeric spike protein, while scanning the human host-cells, is indicated by true (✓, green background, no clash)/false (✗, red background, observed clashes) symbols. The analysis was performed according to the superimposition instructions described in the methods, by using the four conformations according to the available crystallized structures of the SARS-CoV-2 spike protein (6xm5.pdb, showing the 3 RBD in down-conformation, 7kmz.pdb, showing 2 RBD in up and 1 RBD in down-conformation; 7kms. pdb, showing 3 RBD in up-conformation; 6zxn.pdb, showing 2 RBD in down- and 1 RBD in up-conformation). Orange or cyan background indicates nb or derived nb (obtained from the ab FAB portions, see methods) able to simultaneously target three RBD within an entire trimeric spike protein. ab, antibodies; nb, nanobodies; RBD, receptor binding domain; SARS-CoV-2, severe acute respiratory syndrome coronavirus 2.

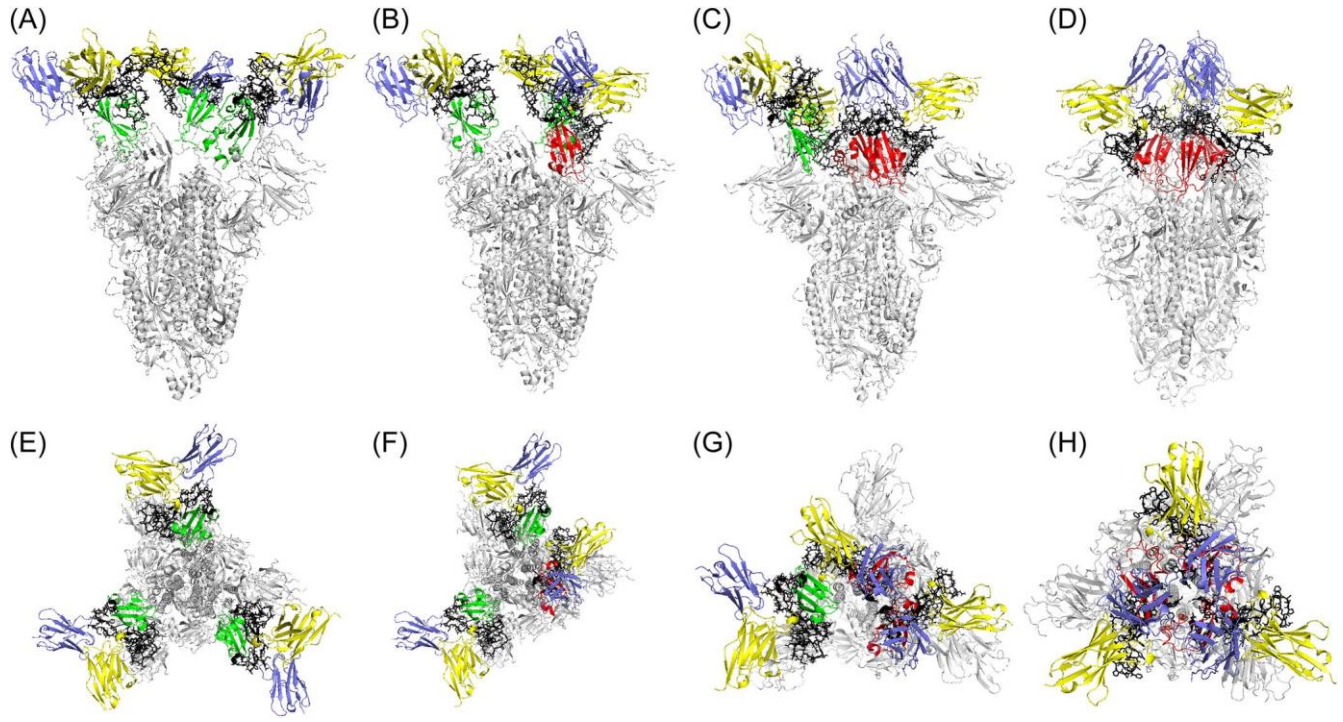

FIGURE 9 Superimposed structures of the proposed REGN10987-LY-CoV555 derived nb combination interacting with the spike RBD on the entire trimeric spike protein in the different investigated conformations, with the best-predicted interaction energy calculated by FOLDX4 plug-in implemented in the Yasara package. The three spike RBD from the entire trimeric spike protein in the four investigated states are reported in red cartoon for RBD (residues 367–518) in down-conformation or in green cartoon for RBD in up-conformation, whereas the RBM residues (amino acids 437–506 of the boat-shaped RBD region) within the three RBD are reported in black cartoon and sticks. (A–D) Show the lateral views of the trimeric spike protein in white cartoon with 3 RBD in up-conformation (A, corresponding to the trimeric spike protein in open conformation, according to 7kms.pdb), 2 RBD in up and 1 RBD in down-conformation (B, according to 7kmz.pdb), 2 RBD in down and 1 RBD in up-conformation (C, according to 6zxn.pdb); 3 RBD in down-conformation (D, corresponding to the trimeric spike protein in close conformation, according to 6xm5.pdb). Similarly, (E)–(H) show the top views of structures described for (A)–(D). The REGN10987 derived nb (from 6xdg.pdb) and the LY-CoV555 derived nb (from 7kmg.pdb) were obtained by truncating the heavy chains of the corresponding crystallized FAB portions at residue 123 (according to REGN10933 sequence numbering, see the "*" column of Figure 3) and are reported in prussian-blue and yellow, respectively, cartoon representation. RBD, receptor binding domain; SARS-CoV-2, severe acute respiratory syndrome coronavirus 2.

target simultaneously all the RBD in a trimeric spike protein, while it assumes the four investigated conformations.

This analysis revealed that only REGN10987 and LY-CoV555 derived nb (i.e., the truncated heavy chains of the cited ab FAB portions, see Figure 3) can target simultaneously the three RBD on the entire spike protein in the four conformations, without creating clashes (Figures 8 and 9).

Considering that the investigated nb H11-H4 (from 6zh9.pdb), Ty1 (from 6zxn.pdb), and Ly-CoV555 (7kmg.pdb) target the same binding region (i.e., the hull region), while REGN10987 (6xdg.pdb) target the stern binding region, the nb and the derived nb were combined to estimate their affinity for the RBD, to propose a "nb/derived nb" cocktail more efficient than the parental nb/ab in preventing spike/ACE2 interactions. This analysis reveals that the three "nb" combinations are able to target simultaneously the three RBD on the spike protein, without creating clashes with the spike body or with adjacent RBD (i.e., when the spike is in the close conformation). In addition, the combination of the REGN10987and Ly-CoV555 derived nb establishes the strongest interactions with the spike RBD (Figure 9 and Table 4), compared to interactions established by the REGN10987/H11-H4 or REGN10987/Ty1 combinations. Furthermore, it is observed that the REGN10987/Ly-CoV555 derived nb combination is the nb combination with the lowest likelihood to form inter-nb clashes along the spike conformational changes and thus, it is believed that such a combination would be very efficient in preventing spike/ACE2 binding interactions.

3.7 | Interaction energy at the protein–protein interface in the protein complexes hosting the Wuhan spike RBD and the investigated nb combined with putative nb derived by the FAB portions of the investigated ab, able to bind more than one RBD on the Wuhan trimeric spike protein in the four investigated spike conformations

More in detail, Figure 9 shows how the combination of ab/nb based on the heavy chains of REGN10987 (from 6xdg.pdb) and

TABLE 4 Free energy of interaction at the spike RBD/nb (derived nb) protein–protein interface.

Pdb	SARS-CoV-2 spike RBD (ch.E) vs LY-CoV555 (ch.A) derived nb/ REGN10987 (ch.C) derived nb	SARS-CoV-2 spike RBD (ch.E) vs H11.H4 (ch.F) derived nb/ REGN10987 (ch.C) derived nb	SARS-CoV-2 spike RBD (ch.E) vs Ty1 (ch.B) derived nb/REGN10987 (ch.C) derived nb
Group 1	AC	CF	BC
Group 2	E	E	E
Intraclashes group 1	12.0	12.3	13.4
Intraclashes group 2	5.4	6.2	6.1
Interaction energy (kcal/mol)	−23.9	−23.3	−21.3
Backbone H-bond	−6.4	−4.1	−4.9
Sidechain H-bond	−10.9	−9.0	−9.1
Van der Waals	−22.8	−19.9	−25.2
Electrostatics	−2.3	−2.3	−0.9
Solvation polar	29.6	25.9	32.9
Solvation hydrophobic	−30.1	−26.3	−33.0
Van der Waals clashes	0.6	0.2	1.9
entropy sidechain	12.4	7.7	10.9
entropy mainchain	5.8	4.9	6.1
torsional clash	0.6	0.2	0.4
backbone clash	4.2	4.1	4.2
disulfide	0.0	0.0	0.0
electrostatic kon	−0.4	−0.4	−0.4
energy ionization	0.0	0.0	0.0
Entropy complex	2.4	2.4	2.4
Number of residues	446	444	435
Interface residues	64	52	67

Note: Please, note that more negative "interaction energy" value indicate stronger binding interactions and thus higher binding affinity at the protein–protein interface of the indicated SARS-CoV-2 spike RBD/nb (derived nb) protein complexes.[2,3,47,55] The energy terms and contributions are reported in kcal/mol according to FOLDX indications. Each energy term has a specific weight in the calculation of the interaction energy, according to the equations previously described.[2,3,47,55] The calculated energy terms and item names are reported in the first cell of each row (i.e., in the first column of the reported table), whereas items (protein names, chain-ID, or protein PDB accession codes) and the calculated energy terms are reported within columns 2–4. The energy terms and contributions are reported in kcal/mol according to FOLDX indications. For a complete explanation of item names and energy terms, please, visit the link http://foldxsuite.crg.eu/command/AnalyseComplex. Interaction energies are also reported in kJ/mol (1 kcal = 4.184 kJ).
Abbreviations: RBD, receptor binding domain; SARS-CoV-2, severe acute respiratory syndrome coronavirus 2.

LY-CoV555 (from 7kmg.pdb) FAB portions, truncated in correspondence of residue number 123 (according to REGN10933 sequence numbering, see the "*" column of Figure 3) might target the three RBD of the spike protein in the investigated four different main conformations, without creating undesired clashes between the three spike monomers (Figure 9). The REGN10987/ LY-CoV555 combination shows the lowest free energy of interaction among the three investigated derived nb combinations (Table 4).

4 | DISCUSSION

The computational pipeline[3] previously provided to build SARS-CoV-2 spike RBD/ACE2 protein complexes, for estimating the SARS-CoV-2 spike affinity for the human ACE2 receptor, for existing and future variants, has now been implemented to build reliable 3D models of the spike protein in complex with ab or nb, starting from a set of ab/nb crystallized in complex with the Wuhan SARS-CoV-2 spike or with the Omicron SARS-CoV-2 spike protein.

The analysis of the spike/ab or spike/nb protein complexes through computational 3D modeling approaches, already validated for different protein targets,[2,3,34,35,50,52–54] has allowed in this case to highlight four preferred RBD regions targeted by the investigated ab/nb. These four regions are located on the RBD surface, forming a boat-shaped area, that largely overlaps with the RBD region involved in interactions with ACE2.[2,3] The SARS-CoV-2 spike/ab and spike/nb crystallized protein complexes were used to calculate the free energy of interaction at the spike RBD/ab or at the spike RBD/nb protein–protein interface of the same crystallized structures. The calculated free energy of interaction obtained from the crystallized structures was used as a reference parameter to establish how the investigated spike variants, modeled by in silico site-directed mutagenesis (within the established modular molecular framework[3]), can form stronger or weaker interactions with the same ab/nb, providing clues about ab/nb efficiency in targeting the spike RBD of new variants, for estimating the ability of new variants in escaping ab/nb. We focused our analyses on interactions between the spike RBD and ab/nb or ACE2, because it was observed that the SARS-CoV-2 spike RBD represents one of the main targets of SARS-CoV-2 neutralizing antibodies, which, as observed, may bind different portions of the RBD. In addition, it was also observed that mutations at the RBD can determine a different ability in the virus to form weaker/stronger interactions with the human ACE2 receptor and/or with the investigated ab/nb,[2,3] mediating a less/more efficient virus entry into the host cells or more/less efficient virus ab escape.

From the performed analysis, it was observed that ab/nb targeting the hull-region of the boat-shaped area form the tightest interactions with the targeted RBD region, suggesting that future ab/nb targeting this region should have a higher chance of success in preventing RBD/ACE2 interactions.

At the same time, it can be argued that knowing mutations at the highlighted four regions of the spike protein of future variants can help in predicting either the spike affinity for ACE2 or putative newly acquired virus escape abilities from the investigated ab/nb (to be modeled according to our modular molecular framework[2,3]), allowing to gain clues about transmissibility and risk associated to the spread of new variants.

As a general trend and, at the same time, as a validation of our computational pipeline, it was indeed observed that new variants show lower binding affinities (according to the calculated free energies of interaction) both towards the human ACE2 (compared to previous estimations against older variants[2,3]) and the investigated ab/nb known to be more efficient against older variants. As an example, the investigated ab and nb show for the spike RBD of the investigated Omicron variants the lowest affinity (in terms of free energy of interactions) most likely because of the discussed mutations detected on the boat-shaped area of the RBD.

4.1 | Considerations about the binding affinity of the investigated ab/nb towards the spike protein

Among the investigated ab used in clinics and/or isolated from patients, such as REGN10933, REGN10987, LY-Cov481, LY-CoV488, LY-CoV555, it is noticed that the investigated REGN-ab target two different regions, namely the stern and the hull-region of the boat-shaped RBD area, whereas the investigated Ly-ab target the hull/hull* region. More in general, it is noticed that the FAB portions of Beta27 and Ly-CoV488, among the investigated ab/nb, show the highest affinity, namely the lowest free energy of interaction, for the spike RBD of most of the investigated variants, including Omicron variants. Among the investigated nb, the VHH_E performs better, by forming strong interactions with residues of the hull binding region on the RBD from the investigated variants. Conversely, nb and ab targeting other regions of the boat-shaped area show weaker affinity, as observed from the calculated free energy of interactions.

4.2 | Clues for improving performances of future ab/nb directed against the spike protein from existing and future variants

Our computational pipeline allows to perform in silico site-directed mutagenesis of ab/nb residues directly within the established molecular framework hosting the RBD/ab or the RBD/nb protein complexes, according to the spike sequences of the investigated variants, aiming to increase their binding affinity towards the spike RBD of existing and future SARS-CoV-2 variants, as long as their sequences become available.[3] The resulting 3D models within the entire molecular framework can be energetically minimized and optimized for allowing a better re-orientation of the side chains of residues at the nb/RBD protein–protein interface to solve minor clashes. Nevertheless, it is worth noting that, to investigate larger conformational changes at the nb/RBD protein–protein interface, a larger session of molecular dynamics analysis should be conducted. As the site-directed mutagenesis is performed, the binding affinity at the protein/protein interface in the new generated 3D protein complexes, can be quickly quantified by Foldx, according to our established protocols.[2,3] A comparative analysis that includes the corresponding binding affinity parameters obtained with older variants will then make possible to predict the affinity of the engineered ab/nb for existing/future RBD variants, providing indications for timely counteracting new virus outbreaks.[3]

4.3 | Nb and derived nb cocktails

In addition, the employed molecular framework has allowed us to analyse how the investigated nb or the “FAB” portions of the investigated ab bind the entire trimeric spike protein. This analysis highlighted a significant limitation of the studied ab/nb, which appear to be not able to target the flexible RBD along all the conformations assumed by the spike protein while scanning host-cell surface.[1,4] It should be stressed that in our molecular framework we used only the FAB portions (the only available on the PDB) of the investigated ab, instead of the entire ab, which will surely generate even more clashes

either between the three spike protein monomers and the antibody or between different antibody units targeting different spike monomers (Figures S1 and S2).

Assuming that the spike protein can show the three RBD in up-conformation (according to 7kms.pdb), in down-conformation (according to 6xm5.pdb), 2 RBD in up- and 1 RBD in down-conformation (according to 7kmz.pdb), 2 RBD in down- and 1 RBD in up-conformation (according to 6zxn.pdb), it was ascertained that 6 out of the 14 investigated ab (FAB portions) and 2 nb out of the 5 investigated nb, cannot target an RBD in up-conformation, if the other two RBD in the trimeric spike protein are in down-conformation, due to the formation of clashes. More in general, our analysis showed that none of the investigated ab was able to bind simultaneously the three RBD of the spike protein independently on their conformation, although we used only the FAB portions of the investigated ab in the generation of the 3D protein complexes. More in detail, clashes between the investigated FAB portions and the spike body and/or adjacent RBD were observed for CR3022, CoVa1.16, LyCoV488, and LyCoV481, when the RBD/ab (FAB portions) were superimposed on the RBD of the entire trimeric spike protein. Clashes among the EY6A/spike RBD complex with adjacent RBD were also observed when the RBD/EY6A protein complex was superimposed on the trimeric entire spike protein showing the 3 RBD in down-conformation or 1 RBD in up- and 2 RBD in down-conformation.

Some RBD regions, as the "stern" and the "rudder*" portions of the boat-shaped RBD surface, due to their locations and to spike conformational changes, cannot be accessed at all by the investigated ab FAB portions directed towards the "stern/rudder*" area, when the RBD are all in down-conformation.

More in general, except for LyCoV555 and CV503, all the other investigated ab cannot target anyu of the three RBD, if the spike protein shows all the RBD in down-conformation, making slower the recognition of the circulating virus.

Remarkably, while some ab (i.e., REGN10987 or Beta55, Figure 8) appear able to target two different RBD in up- conformation, also while interacting with a spike protein showing 2RBD in up- and 1 RBD in down-conformation without creating ab/ RBD clashes with adjacent RBD, bad clashes can be observed between the different ab chains targeting adjacent RBD of a trimeric spike protein, in presence of most of the investigated ab targeting aspike protein showing 2 RBD in up- and 1 RBD in down- conformation (i.e., as observed for CoVa1.16, CR3022, and LyCoV488, Figure 8).

If the entire ab would be used in place of the employed FAB portions, it is expected that the targeting of the entire trimeric spike protein would be even more difficult due to the steric hindrance of the entire ab that will increase the likelihood to create clashes with close regions of adjacent spike monomer or between close ab chains targeting different spike monomers (see Beta27 in Figure S2).

Considering the above-reported observations, it is more difficult to imagine an efficient ab/nb cocktail able to target more than one RBD on the same trimeric spike protein, while the spike protein assumes the different investigated conformations, along its dynamical scanning of the host-cell surface. Indeed, it is believed that the spike flexibility and the high mobility of the spike RBD confers to the SARS-CoV-2 the ability to avoid/prevent or reduce/disadvantage interactions with the large entire structure of an ab.[1,4]

On the other hand, in our analysis it was observed that 2 out of the 5 investigated nb, namely H11-H4 and Ty1, were able to bind simultaneously the three RBD of the spike protein independently on the spike conformation. This ability was related both to the specific targeted RBD "hull" region, and also to the nb smaller size.

Thus, it is expected that nb with high affinity for the spike RBD, able to simultaneously target the three RBD of a trimeric spike protein, independently on the assumed conformation, may provide a more effective weapon to deal with infections related to viruses using a spike-like protein for invading host-cells, in the future.

To prove this hypothesis, we truncated the heavy chains of the investigated FAB to derive an ideal nb, to be tested in combination with the other investigated nb, searching for the best combination to target simultaneously the three RBD on the flexible, highly mobile, trimeric spike protein in the different investigated conformations, without creating clashes at the nb/nb interface or among nb and adjacent RBD.

Thus, among the investigated nb and derived nb, the nb H11-H4 (from 6zh9.pdb) and Ty1 (from 6zxn.pdb), together with the nb derived from LY-CoV555 nb (7kmg.pdb), targeting the "hull" region of the boat-shaped RBD surface, and the nb derived from REGN10987 (6xdg.pdb), targeting the "stern" binding region of the boat-shaped surface, appear to be the ideal candidates to be combined to propose a "nb" cocktail more efficient than the parental nb/ab in preventing spike/ACE2 interactions.

Notably, this analysis revealed that the three "nb" cocktails, resulting from the combination of the above–cited nb and/or derived nb, can target simultaneously the three RBD on the spike protein, without creating inter nb clashes, or clashes with the spike body or with adjacent RBD, independently on the investigated four conformations that the spike protein can assume by scanning the host cell-surface.

Furthermore, the combination of the REGN10987/LY-CoV555 derived nb combination appears to be the ones that forms slightly more stable interactions with the spike RBD, compared to interactions established by the REGN10987/H11-H4 or REGN10987/Ty1 combinations, and at the same time the REGN10987/LY-CoV555 derived nb combination appears the one with the lowest likelihood to form inter-nb clashes, while the spike protein undergoes conformational changes.

In conclusion, in light of all the above–reported observations, we may propose that a cocktail of nb, instead of ab, targeting the "hull" and the "stern" region of the spike RBD, as observed for the REGN10987/Ly-CoV555 derived nb combination (but also for the REGN10987/H11-H4 and the REGN10987/Ty1 derived nb/nb combinations), would be more efficient than previously described ab/ab or ab/nb cocktails in preventing spike RBD/ACE2 interactions and virus infection.

LIST OF THE ANALYSED SARS-COV-2 VARIANTS AND LINK TO THE OUTBREAK.INFO DATABASE FOR MUTATION PREVALENCE

hCoV-19/Wuhan/WIV04/2019, YP_009724390.1; Gisaid: EPI_ISL_402124 (see "clade evolution in the first year" on https://www.gisaid.org/);

B.1.1.7-United-Kingdom; https://outbreak.info/compare-lineages?pango=B.1.1.7&gene=S&threshold=0.2;

P.1-Japan/Brazil; https://outbreak.info/compare-lineages?pango=P.1%3B&gene=S&threshold=0.2;

B.1.351-South Africa; https://outbreak.info/compare-lineages?pango=B.1.351%3B&gene=S&threshold=0.2;

B.1.427/B.1.429-California; https://outbreak.info/compare-lineages?pango=B.1.427%3B&gene=S&threshold=0.2;

B.1.141; https://cov-lineages.org/lineage.html?lineage=B. 1.141; also referred to as B.1.466.2 or B.1.258.22: https://outbreak.info/compare-lineages?pango=B.1.258.22&gene=S&threshold=0.2;

B.1.617.1-India; https://outbreak.info/compare-lineages?pango=B.1.617&gene=S&threshold=0.2;

B.1.620; https://outbreak.info/compare-lineages?pango=B.1.620%3B&gene=S&threshold=0.2; for a complete list of the investigated mutations see: https://covdb.stanford.edu/page/mutation-viewer; or https://www.ncbi.nlm.nih.gov/lab/virus/vssi/#/scov2_snp;

B.1.1.529; https://outbreak.info/situation-reports?xmin=2022-08-16&xmax=2023-02-16&pango=B.1.1.529;

BA.4/5; https://outbreak.info/situation-reports?xmin=2022-08-16&xmax=2023-02-16&pango=BA.5.

AUTHOR CONTRIBUTIONS

Conceptualization: Ciro Leonardo Pierri. *Data curation*: Vincenzo Tragni, Ivan Mercurio, Diletta Pia Paoletti, Luna Laera, Lucas Cafferati Beltrame, Maria Noemi Sgobba, Angelo Onofrio. *Formal analysis*: Vincenzo Tragni, Ivan Mercurio, Diletta Pia Paoletti, Luna Laera, Angelo Onofrio, Ciro Leonardo Pierri. *Methodology*: Vincenzo Tragni, Ivan Mercurio, Diletta Pia Paoletti, Luna Laera, Lucas Cafferati Beltrame, Maria Noemi Sgobba, Angelo Onofrio, and Ciro Leonardo Pierri. *Supervision*: Gabriella Elia, Mariateresa Volpicella, Lorenzo Guerra, Anna De Grassi, and Ciro Leonardo Pierri. *Writing—original draft*: Vincenzo Tragni, Ivan Mercurio, Diletta Pia Paoletti, and Ciro Leonardo Pierri. *Writing—review and editing*: Vincenzo Tragni, Luna Laera, Diletta Pia Paoletti, Angelo Onofrio, Ivan Mercurio, Gabriella Elia, Mariateresa Volpicella, Anna De Grassi, Lorenzo Guerra, and Ciro Leonardo Pierri.

ACKNOWLEDGMENTS

This research was supported by EU funding within the MUR PNRR Extended Partnership initiative on Emerging Infectious Diseases (Project no. PE00000007, INF-ACT) and MUR PNRR National Center for Gene Therapy and Drugs based on RNA Technology (Project no. CN_00000041). The authors would also like to thank for the IT resources made available by ReCaS (https://www.recas-bari.it/index.php/en/), a project funded by the MIUR (Italian Ministry for Education, University and Re-search) in the "PON Ricerca e Competitivita 2007–2013-Azione I-Interventi di rafforzamento strutturale" PONa3_00052, Avviso 254/Ric, University of Bari. In addition, the authors would like to thank the Italian Association for Mitochondrial Research (www.mitoairm.it) for providing part of the computational resources.

CONFLICT OF INTEREST STATEMENT

The authors declare no conflicts of interest.

DATA AVAILABILITY STATEMENT

The data that support the findings of this study are available from the corresponding author upon reasonable request. Data will be made available on request.

ORCID

Ciro Leonardo Pierri http://orcid.org/0000-0003-1816-548X

REFERENCES

1. Pierri CL. SARS-CoV-2 spike protein: flexibility as a new target for fighting infection. *Signal Transduct Target Ther*. 2020;5(1):254. doi:10.1038/s41392-020-00369-3
2. Mercurio I, Tragni V, Busto F, De Grassi A, Pierri CL. Protein structure analysis of the interactions between SARS-CoV-2 spike protein and the human ACE2 receptor: from conformational changes to novel neutralizing antibodies. *Cell Mol Life Sci*. 2021;78: 1501-1522. doi:10.1007/s00018-020-03580-1
3. Tragni V, Preziusi F, Laera L, et al. Modeling SARS-CoV-2 spike/ACE2 protein–protein interactions for predicting the binding affinity of new spike variants for ACE2, and novel ACE2 structurally related human protein targets, for COVID-19 handling in the 3PM context. *EPMA J*. 2022;13(1):149-175. doi:10.1007/s13167-021-00267-w
4. Turoňová B, Sikora M, Schürmann C, et al. In situ structural analysis of SARS-CoV-2 spike reveals flexibility mediated by three hinges. *Science*. 2020;370:203-208. doi:10.1126/science.abd5223
5. Wrapp D, Wang N, Corbett KS, et al. Cryo-EM structure of the 2019-nCoV spike in the prefusion conformation. *Science*. 2020;367(6483):1260-1263. doi:10.1126/science.abb2507
6. Hoffmann M, Kleine-Weber H, Schroeder S, et al. SARS-CoV-2 cell entry depends on ACE2 and TMPRSS2 and is blocked by a clinically proven protease inhibitor. *Cell*. Published online 2020;181: 271-280.e8. doi:10.1016/j.cell.2020.02.052
7. Walls AC, Park YJ, Tortorici MA, Wall A, McGuire AT, Veesler D. Structure, function, and antigenicity of the SARS-CoV-2 spike glycoprotein. *Cell*. 2020;181(2):281-292.e6. doi:10.1016/j.cell.2020.02.058
8. Warwicker J. A model for pH coupling of the SARS-CoV-2 spike protein open/closed equilibrium. *Brief Bioinform*. 2021;22(2): 1499-1507. doi:10.1093/bib/bbab056
9. Zhou T, Tsybovsky Y, Gorman J, et al. Cryo-EM structures of SARS-CoV-2 spike without and with ACE2 reveal a pH-Dependent switch to mediate endosomal positioning of receptor-binding domains. *Cell Host Microbe*. 2020;28(6):867-879.e5. doi:10.1016/j.chom.2020.11.004
10. Heinz FX, Stiasny K. Distinguishing features of current COVID-19 vaccines: knowns and unknowns of antigen presentation and modes of action. *NPJ Vaccines*. 2021;6:104. doi:10.1038/s41541-021-00369-6
11. Greaney AJ, Loes AN, Crawford KHD, et al. Comprehensive mapping of mutations in the SARS-CoV-2 receptor-binding domain that

affect recognition by polyclonal human plasma antibodies. *Cell Host Microbe*. 2021;29:463-476.e6. doi:10.1016/j.chom.2021.02.003
12. Thomson EC, Rosen LE, Shepherd JG, et al. Circulating SARS-CoV-2 spike N439K variants maintain fitness while evading antibody-mediated immunity. *Cell*. 2021;184:1171-1187.e20. doi:10.1016/j.cell.2021.01.037
13. Zhou D, Dejnirattisai W, Supasa P, et al. Evidence of escape of SARS-CoV-2 variant B.1.351 from natural and vaccine-induced sera. *Cell*. 2021;184:2348-2361.e6. doi:10.1016/j.cell.2021.02.037
14. Planas D, Bruel T, Grzelak L, et al. Sensitivity of infectious SARS-CoV-2 B.1.1.7 and B.1.351 variants to neutralizing anti- bodies. *Nature Med*. 2021;27:917-924. doi:10.1038/s41591-021- 01318-5
15. Hansen J, Baum A, Pascal KE, et al. Studies in humanized mice and convalescent humans yield a SARS-CoV-2 antibody cocktail. *Science*. 2020;369(6506):1010-1014. doi:10.1126/science.abd0827.
16. Kim C, Ryu DK, Lee J, et al. A therapeutic neutralizing antibody targeting receptor binding domain of SARS-CoV-2 spike protein. *Nat Commun*. 2021;12(1):288. doi:10.1038/s41467-020-20602-5
17. Hanke L, Vidakovics Perez L, Sheward DJ, et al. An alpaca nanobody neutralizes SARS-CoV-2 by blocking receptor interaction. *Nat Commun*. 2020;11(1):4420. doi:10.1038/s41467-020-18174-5
18. McCallum M, Bassi J, De Marco A, et al. SARS-CoV-2 immune evasion by the B.1.427/B.1.429 variant of concern. *Science*. 2021;373(6555):648-654. doi:10.1101/2021.03.31.437925
19. Zou J, Kurhade C, Patel S, et al. Neutralization of BA.4-BA.5, BA.4.6, BA.2.75.2, BQ.1.1, and XBB.1 with bivalent vaccine. *N Engl J Med*. 2023;388:854-857. doi:10.1056/NEJMc2214916
20. Lamb YN. Nirmatrelvir plus ritonavir: first approval. *Drugs*. 2022;82:585-591. doi:10.1007/s40265-022-01692-5
21. Jayk Bernal A, Gomes da Silva MM, Musungaie DB, et al. Molnupiravir for oral treatment of Covid-19 in nonhospitalized patients. *N Engl J Med*. 2022;386:509-520. doi:10.1056/nejmoa2116044
22. Reis G, dos Santos Moreira-Silva EA, Silva DCM, et al. Effect of early treatment with fluvoxamine on risk of emergency care and hospitalisation among patients with COVID-19: the TOGETHER randomised, platform clinical trial. *Lancet Glob Heal*. 2022;10(1): e42-e51. doi:10.1016/S2214-109X(21)00448-4
23. Wen W, Chen C, Tang J, et al. Efficacy and safety of three new oral antiviral treatment (molnupiravir, fluvoxamine and Paxlovid) for COVID-19:a meta-analysis. *Ann Med*. 2022;54(1):516-523. doi:10.1080/07853890.2022.2034936
24. Abraham J. Monoclonal antibodies with extended half-life to prevent Covid-19. *N Engl J Med*. 2022;386(23):2236-2238. doi:10.1056/NEJME2205563
25. Huo J, Le Bas A, Ruza RR, et al. Neutralizing nanobodies bind SARS-CoV-2 spike RBD and block interaction with ACE2. *Nat Struct Mol Biol*. 2020;27(9):846-854. doi:10.1038/s41594-020-0469-6
26. Jones BE, Brown-Augsburger PL, Corbett KS, et al. The neutralizing antibody, LY-CoV555, protects against SARS-CoV-2 infection in nonhuman primates. *Sci Transl Med*. 2021;13(593):1-18. doi:10.1126/scitranslmed.abf1906
27. Koenig PA, Das H, Liu H, et al. Structure-guided multivalent nanobodies block SARS-CoV-2 infection and suppress mutational escape. *Science*. 2021;371(6530):eabe6230. doi:10.1126/science.abe6230
28. Prabakaran P, Gan J, Feng Y, et al. Structure of severe acute respiratory syndrome coronavirus receptor-binding domain complexed with neutralizing antibody. *J Biol Chem*. 2006;281(23):15829-15836. doi:10.1074/jbc.M600697200
29. Wu NC, Yuan M, Bangaru S, et al. A natural mutation between SARS-CoV-2 and SARS-CoV determines neutralization by a cross- reactive antibody. *PLoS Pathog*. 2020;16(12):e1009089. doi:10.1371/journal.ppat.1009089
30. Cho H, Gonzales-Wartz KK, Huang D, et al. Bispecific antibodies targeting distinct regions of the spike protein potently neutralize SARS-CoV-2 variants of concern. *Sci Transl Med*. 2021;13(616):eabj5413. doi:10.1126/scitranslmed.abj5413
31. Yuan M, Zhu X, He W, et al. A broad and potent neutralization epitope in SARS-related coronaviruses. *Proc Natl Acad Sci USA*. 2022;119(29):e2205784119. doi:10.1073/pnas.2205784119
32. Tuekprakhon A, Nutalai R, Dijokaite-Guraliuc A, et al. Antibody escape of SARS-CoV-2 Omicron BA.4 and BA.5 from vaccine and BA.1 serum. *Cell*. 2022;185:2422-2433.e13. doi:10.1016/j.cell.2022.06.005
33. Dejnirattisai W, Huo J, Zhou D, et al. SARS-CoV-2 Omicron-B.1.1.529 leads to widespread escape from neutralizing antibody responses. *Cell*. 2022;185:467-484.e15. doi:10.1016/j.cell.2021.12.046
34. Pierri CL, Bossis F, Punzi G, et al. Molecular modeling of antibodies for the treatment of TNF*a*-related immunological diseases. *Pharmacol Res Perspect*. 2016;4(1):e00197. doi:10.1002/prp2.197
35. Trisolini L, Gambacorta N, Gorgoglione R, et al. FAD/NADH dependent oxidoreductases: from different amino acid sequences to similar protein shapes for playing an ancient function. *J Clin Med*. 2019;8(12):2117. doi:10.3390/jcm8122117
36. Chiara M, D'Erchia AM, Gissi C, et al. Next generation sequencing of SARS-CoV-2 genomes: challenges, applications and opportunities. *Brief Bioinform*. 2021;22:616-630. doi:10.1093/bib/bbaa297
37. Chiara M, Zambelli F, Tangaro MA, Mandreoli P, Horner DS, Pesole G. CorGAT: a tool for the functional annotation of SARS- CoV-2 genomes. *Bioinformatics*. 2021;36:5522-5523. doi:10.1093/bioinformatics/btaa1047
38. Yadav PD, Sapkal GN, Abraham P, et al. Neutralization of variant under investigation B.1.617.1 with sera of BBV152 vaccinees. *Clin Infect Dis*. 2021;74(2):366-368. doi:10.1093/cid/ciab411
39. Frampton D, Rampling T, Cross A, et al. Genomic characteristics and clinical effect of the emergent SARS-CoV-2 B.1.1.7 lineage in London, UK: a whole-genome sequencing and hospital-based cohort study. *Lancet Infect Dis*. 2021;21:1246-1256. doi:10.1016/s1473-3099(21)00170-5
40. Hirotsu Y, Omata M. Discovery of a SARS-CoV-2 variant from the P.1 lineage harboring K417T/E484K/N501Y mutations in Kofu, Japan. *J Infect*. 2021;82:276-316. doi:10.1016/j.jinf.2021.03.013
41. Nyberg T, Ferguson NM, Nash SG, et al. Comparative analysis of the risks of hospitalisation and death associated with SARS-CoV-2 omicron (B.1.1.529) and delta (B.1.617.2) variants in England: a cohort study. *The Lancet*. 2022;399(10332):1303-1312. doi:10.2139/ssrn.4025932
42. Lan J, Ge J, Yu J, et al. Structure of the SARS-CoV-2 spike receptor-binding domain bound to the ACE2 receptor. *Nature*. 2020;581:215-220. doi:10.1038/s41586-020-2180-5
43. Mannar D, Saville JW, Zhu X, et al. SARS-CoV-2 Omicron variant: antibody evasion and cryo-EM structure of spike protein–ACE2 complex. *Science*. 2022;375(6582):760-764. doi:10.1126/science.abn7760
44. Kimura I, Yamasoba D, Tamura T, et al. Virological characteristics of the SARS-CoV-2 Omicron BA.2 subvariants, including BA.4 andBA.5. *Cell*. 2022;185(21):3992-4007.e16. doi:10.1016/j.cell.2022. 09.018
45. Persson B. Bioinformatics in protein analysis. In: *Proteomics in Functional Genomics*. Vol 88. Birkhäuser Basel; 2000:215-231. doi:10.1007/978-3-0348-8458-7_14
46. Waterhouse AM, Procter JB, Martin DMA, Clamp M, Barton GJ. Jalview version 2-A multiple sequence alignment editor and analysis workbench. *Bioinformatics*. 2009;25(9):1189-1191. doi:10.1093/bioinformatics/btp033
47. Schymkowitz J, Borg J, Stricher F, Nys R, Rousseau F, Serrano L. The FoldX web server: an online force field. *Nucleic Acids Res*. 2005;33(Web Server issue):W382-W388. doi:10.1093/nar/gki387

48. Krieger E, Joo K, Lee J, et al. Improving physical realism, stereochemistry, and side-chain accuracy in homology modeling: four approaches that performed well in CASP8. *Proteins: Struct, Funct, Bioinf*. 2009;77(S9):114-122. doi:10.1002/prot.22570
49. Chen J, Gao K, Wang R, Wei GW. Revealing the threat of emerging SARS-CoV-2 mutations to antibody therapies. *J Mol Biol*. 2021;433(18):167155. doi:10.1016/j.jmb.2021.167155
50. Pierri CL, Parisi G, Porcelli V. Computational approaches for protein function prediction: a combined strategy from multiple sequence alignment to molecular docking-based virtual screening. *Biochimica et Biophysica Acta (BBA) - Proteins and Proteomics*. 2010;1804(9): 1695-1712. doi:10.1016/j.bbapap.2010.04.008
51. Ordog R. PyDeT, a PyMOL plug-in for visualizing geometric concepts around proteins. *Bioinformation*. 2008;2(8):346-347.
52. Bossis F, De Grassi A, Palese LL, Pierri CL. Prediction of high- and low-affinity quinol-analogue-binding sites in the aa3and bo3 terminal oxidases from Bacillus subtilis and *Escherichia coli*. *Biochem J*. 2014;461(2):305-314. doi:10.1042/BJ20140082
53. Shteyer E, Edvardson S, Wynia-Smith SL, et al. Truncating mutation in the nitric oxide synthase 1 gene is associated with infantile achalasia. *Gastroenterology*. 2015;148(3):533-536.e4. doi:10.1053/j.gastro.2014.11.044
54. Ta-Shma A, Pierri CL, Stepensky P, et al. Isolated truncus arteriosus associated with a mutation in the plexin-D1 gene. *Am J Med Genet, Part A*. 2013;161(12):3115-3120. doi:10.1002/ajmg.a.36194
55. Van Durme J, Delgado J, Stricher F, Serrano L, Schymkowitz J, Rousseau F. A graphical interface for the FoldX forcefield. *Bioinformatics* . 2011; 27(12):1711 - 1712. doi:10.1093/bioinformatics/btr254
56. Zhou W, Xu C, Wang P, et al. N439K variant in spike protein may alter the infection efficiency and antigenicity of SARS-CoV-2 based on molecular dynamics simulation. *bioRxiv*. 2020;2:5-7. doi:10.1101/2020.11.21.392407
57. Yang HM, Junior LPL, Yang AC. Evaluating the trade-off between transmissibility and virulence of SARS-CoV-2 by mathematical modeling. *medRxiv*. 2021;1-22. doi:10.1101/2021.02.27.21252592
58. Geoghegan JL, Holmes EC. The phylogenomics of evolving virus virulence. *Nat Rev Genet*. 2018;19(12):756-769. doi:10.1038/s41576-018-0055-5
59. Leung NHL. Transmissibility and transmission of respiratory viruses. *Nat Rev Microbiol*. 2021;19(8):528-545. doi:10.1038/s41579-021-00535-6
60. Bálint G, Vörös-Horváth B, Széchenyi A. Omicron: increased transmissibility and decreased pathogenicity. *Signal Transduct Target Ther*. 2022;7(1):151. doi:10.1038/s41392-022-01009-8

SUPPORTING INFORMATION

Additional supporting information can be found online in the Supporting Information section at the end of this article.